Dalton Transactions

Cobalt(II) acyl intermediates in carbon-carbon bond formation and oxygenation

Journal:	*Dalton Transactions*
Manuscript ID	DT-ART-06-2018-002661.R1
Article Type:	Paper
Date Submitted by the Author:	24-Jul-2018
Complete List of Authors:	Reinig, Regina; Iowa State University, Department of Chemistry Fought, Ellie; Iowa State University, Department of Chemistry Ellern, Arkady; Iowa State University of Science and Technology, bMolecular Structure Laboratory Windus, Theresa; Iowa State University, Chemistry Sadow, Aaron; Iowa State University, Department of Chemistry

Dalton Transactions

ARTICLE

Cobalt(II) acyl intermediates in carbon-carbon bond formation and oxygenation

Received 00th January 20xx,
Accepted 00th January 20xx

DOI: 10.1039/x0xx00000x

www.rsc.org/

Regina R. Reinig,[a] Ellie L. Fought, [a] Arkady Ellern,[b] Theresa L. Windus,[a] and Aaron D. Sadow[a]

The organocobalt scorpionate compounds To^{M}CoR (To^{M} = tris(4,4-dimethyl-2-oxazolinyl)phenylborate; R = Bn, **1**; CH_2SiMe_3, **2**; Ph, **3**; Et, **4**; ^{n}Bu, **5**; Me, **6**) react in carbonylation, oxidation, and carboxylation reactions via pathways that are distinctly influenced by the nature of the organometallic moiety. The compounds are prepared by reaction of To^{M}CoCl with the corresponding organolithium or organopotassium reagents. Compounds **1** – **6** were characterized by 8-line hyperfine coupling to cobalt in EPR spectra and solution phase magnetic measurements (μ_{eff} = 4 – 5 μ_B) as containing a high-spin cobalt(II) center. The UV-Vis spectra revealed an intense diagnostic band at ca. 700 nm (ε > 1000 $M^{-1}cm^{-1}$) associated with the tetrahedral organocobalt(II) center that was assigned to a d←d transition on the basis of configuration interaction (CI) calculations. Complexes **1** – **6** react rapidly with CO to form equilibrating mixtures of the low spin organocobalt carbonyl To^{M}Co(R)CO, acyl To^{M}CoC(=O)R, and acyl carbonyl To^{M}Co{C(=O)R}CO. The ^{1}H and ^{11}B NMR spectra contained only one set of signals for the CO-treated solutions, whereas the solution-phase IR spectra contained up to two ν_{CO} and three $\nu_{C(=O)R}$ signals with intensities varying depending on the R group (R = Bn, **7**; CH_2SiMe_3, **8**; Ph, **9**; Et, **10**; ^{n}Bu, **11**; Me, **12**). Single crystal X-ray diffraction of To^{M}Co{C(=O)Et}CO (**10**) supports its assignment as a square pyramidal cobalt(II) acyl carbonyl complex. Upon evaporation of volatiles, solutions of **8** – **12** revert to the CO-free organocobalt starting materials **2** – **6**, whereas attempts to isolate benzyl-derived **7** provide an unusual α-alkoxyketone species, characterized by single crystal X-ray diffraction. Despite the differences observed in the carbonylation of **1** – **6** as a result of varying the R group, compounds **7** – **12** all react rapidly with O_2 through an oxygenation pathway to afford the corresponding carboxylate compounds To$^{M}CoO_2CR$ (R = Bn, **13**; CH_2SiMe_3, **14**; Ph, **15**; Et, **16**; ^{n}Bu, **17**; Me, **18**). In contrast, the insertion of CO_2 into the Co–C bond in **7** – **12** requires several days to weeks.

Introduction

Oxidative carbonylation, an organotransition metal-mediated route to carboxylates, typically proceeds by a sequence in which a metal hydrocarbyl reacts with CO to form an acyl, followed by hydrolysis and reductive elimination. Under catalytic conditions, metal-centered oxidation and metalation steps complete the cycle to generate a new metal hydrocarbyl. This kind of pathway has been proposed for palladium-catalyzed oxidative carbonylation of arenes,[1] as well as catalytic carboxylations of amides to give carbamates and ureas.[2] Remarkably, the biological synthesis of acetate also involves carbonylation of an organometallic nickel methyl to give an acetyl group that is transferred to acetyl Co-A to form a thioacetate and then subsequently hydrolyzed.[3-5] The fact that carbon dioxide, which serves as the source of both carbon atoms in acetate, is not incorporated into acetate by direct insertion into the metal-methyl is perhaps even more remarkable. Instead, CO_2 is reduced both to the methyl and to CO by CO dehydrogenase.[6, 7] Similarly, in synthetic chemistry, the synthesis of acetate or acetic acid via the Monsanto process involves CO, reductive elimination and hydrolysis rather than direct insertion of CO_2.[8] These carbonylations result in oxygenation of an acyl to carboxylate, but the pathways invoke hydrolysis followed by oxidation at the metal center rather than by direct oxygenation of the metal acyl species. The distinction between oxidation catalysis (including reactions mediated by oxidases)[9] and oxygenation catalysis (catalyzed by oxygenases) affects the choice of reagent as the oxygen source and oxidant, as well as the conditions and occasions for their use. Nonetheless, acyl species are proposed as likely intermediates in multiple pathways, therefore identification of the conditions by which acyl metal compounds form and their subsequent reaction pathways are key to developing new transformations.

A seemingly straightforward and well-established route to acyl compounds involves an insertive combination of CO and organometallic compounds. For tetrahedral organometallic compounds, however, a number of species and pathways can result from interactions with CO. In one pathway, the

[a] US Department of Energy Ames Laboratory and Department of Chemistry, 1605 Gilman Hall, Iowa State University, Ames IA 50011, USA.
[b] Department of Chemistry, 1605 Gilman Hall, Iowa State University, Ames IA 50011, USA.

† Dedicated to Professor R. A. Andersen on the occasion of his 75th birthday.
Electronic Supplementary Information (ESI) available: Spectroscopic and computational data. CCDC 1845864 – 1845874. For ESI, see DOI: 10.1039/x0xx00000x See DOI: 10.1039/x0xx00000x

coordination of CO to the metal center gives a metal hydrocarbyl carbonyl adduct, which can undergo insertion to form an isomeric acyl species. Further coordination of one or two CO ligands is likely influenced by the steric properties of the ancillary ligand or acyl group and by the electronic configuration of the metal center. For example, acyl derivatives of $Tp^{R'}CoEt$, $Tp^{R'}CoC_3H_5$ and $Tp^{R'}CoCH_2C_6H_4OMe$ are isolable ($Tp^{R'}$ = Tp^{iPr2} or Tp^{Me3}; Tp^{iPr2} = tris(3,5-diisopropylpyrazolyl)borate; Tp^{Me3} = tris(3,4,5-trimethylpyrazolyl)borate).[10,11]

Alternatively, reactions of tetrahedral divalent organometallics with CO can result in 1 e^- reduction to form carbonyl adducts.[12, 13] Reduction is typically observed with bulky ancillary ligands, such as in the reactions of CO and $Tp^{tBu,Me}CoMe$ ($Tp^{tBu,Me}$ = tris(3-*t*-butyl-5-methylpyrazolyl)borate) or $PhTp^{tBu}FeMe$ ($PhTp^{tBu}$ = tris(3-*t*-butylpyrazolyl)phenylborate) that form cobalt(I) or iron(I) carbonyls, respectively. Homolysis of tetrahedral cobalt alkyls is also proposed as the first step in the rearrangement of $Tp^{Ph,Me}Cot$Bu ($Tp^{Ph,Me}$ = tris(3-phenyl-5-methylpyrazolyl)borate) to $Tp^{Ph,Me}CoCH_2CHMe_2$.[14] Interestingly, $Tp^{R'}CoEt$ and CO provides first the acylcobalt carbonyl species, which forms $Tp^{R'}CoCO$ upon removal of volatiles,[11] and this is suggested to occur by homolysis of $Tp^{R'}CoEt(CO)$. The fate of the organometallic ligand in these reductive pathways has not been established.

Recently, we reported the synthesis of To^MCoMe (To^M = tris(4,4-dimethyl-2-oxazolinyl)phenylborate) by reaction of To^MCoCl with MeLi. To^MCoMe reacts readily with CO to form $To^MCo\{C(=O)Me\}CO$ followed by rapid reaction with O_2 to produce To^MCoOAc.[15] Direct insertion of CO_2 into To^MCoMe also affords To^MCoOAc, but the reaction requires several weeks. The observation that the multistep pathway is, at least in this case, significantly faster than direct insertion, motivated us to expand the study to other organocobalt species supported by To^M to determine if this reactivity is general to other alkyl and aryl groups.

Herein, we prepare a series of alkyl, aryl, and benzyl cobalt(II) compounds supported by a tris(oxazolinyl)borate ligand. The spectroscopic, electronic, and structural features are compared within the series of organocobalt(II) compounds and with halide and pseudo-halide analogues to discover distinguishing features that might parallel reactivity differences within the series of compounds and to related four-coordinate cobalt alkyls. The products of carbonylation are characteristic of the hydrocarbyl ligand, as identified by signals observed in the infrared spectra in carbonyl and acyl C=O stretching regions. These carbonylation products are oxygenated in reactions with O_2, which occurs rapidly, in contrast to sluggish reactions of the organocobalt compounds and carbon dioxide.

Results and discussion

Synthesis and characterization of To^MCoR.

The organometallic cobalt(II) complexes To^MCoR (R = Bn, **1**; CH_2SiMe_3, **2**; Ph, **3**; Et, **4**; ^{n}Bu, **5**; Me, **6**) are prepared by salt metathesis reactions involving To^MCoCl and excess (1.4 – 1.7 equiv.) organopotassium ($PhCH_2K$) or organolithium (Me_3SiCH_2Li, PhLi, EtLi, ^{n}BuLi, MeLi) reagents (Scheme 1).[15] To^MCoMe and To^MCoBn are the most straightforward to prepare and form in good yields at room temperature under dilute conditions. For example, To^MCoBn (**1**, 0.129 g, 0.242 mmol, 79%) is synthesized from To^MCoCl (0.308 mmol, 0.031 M) and 1.7 equiv. of KBn in THF at room temperature.

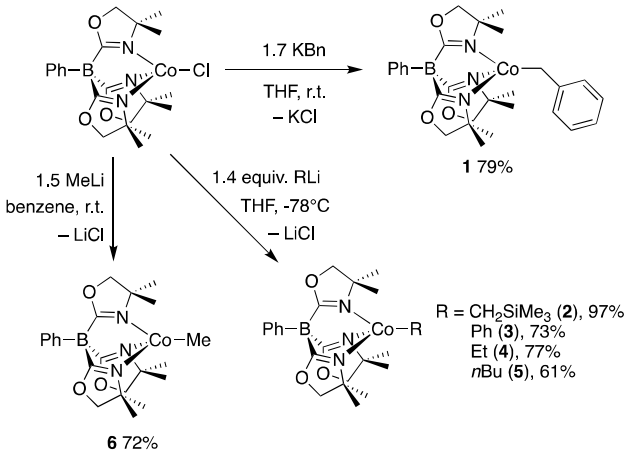

Scheme 1. Synthesis of To^MCoBn (**1**), $To^MCoCH_2SiMe_3$ (**2**), To^MCoPh (**3**), To^MCoEt (**4**), To^MCo^nBu (**5**), and To^MCoMe (**6**).

Dilute conditions (~0.02 M) are also effective on a ~0.03 mmol scale for synthesizing organocobalt(II) complexes **2** – **5** in good yield (>50%). Unfortunately, preparative scale reactions for **2** – **5** (>0.06 mmol) under these dilute conditions consistently give less than 30% yield. Instead, **2** – **5** require more concentrated conditions (~0.1 M) and low temperature reactions. Using 0.1 M To^MCoCl, 1.4 equiv. of alkyllithium, and mixtures cooled to –78 °C, $To^MCoCH_2SiMe_3$ (**2**), To^MCoPh (**3**), To^MCoEt (**4**) and To^MCo^nBu (**5**) are reproducibly synthesized in greater than 0.20 mmol quantities and >60% yields. These conditions provide spectroscopically and analytically pure To^MCoR. Signals for To^MCoCl in NMR and UV-vis spectra, even as a trace impurity, were not detected for these samples (see below).

NMR spectroscopy provided an initial assay for alkyl- or arylation of To^MCoCl. Despite the paramagnetic nature of these cobalt(II) complexes, both ^1H and ^{11}B NMR spectroscopy clearly distinguished To^MCoCl from the organocobalt(II) complexes by their chemical shifts (Table 1). The To^M-based pattern of signals was consistent with C_{3v}-symmetric species, and their chemical shifts appeared in similar regions for all six organocobalt compounds. The signals attributed to the oxazoline methyl groups ranged from –9.6 to –14.5 ppm, which was more than 15 ppm lower frequency compared to the corresponding signal in To^MCoCl at 8.38 ppm. The oxazoline methylene peaks' range was even smaller, from 14.8

– 16.7 ppm, whereas the corresponding resonance in To^{M}CoCl was observed at 24.9 ppm. While the chemical shifts for the To^{M} ligand were similar across **1** – **6**, the detected signals for the alkyl and aryl ligands were wide ranging. For example, the benzyl ligand resonances in **1**, were observed at 34, –77, and –89 ppm. ^{1}H NMR peaks that might be attributed to hydrogen on the α-carbon were not detected in any of the alkyl compounds.

The ^{11}B NMR spectra of these complexes each contained one peak, the chemical shift of which ranged from 87 to 117 ppm. These signals had far higher frequency chemical shifts compared to the resonances of the chloride (–29 ppm) as well as diamagnetic species resulting from transmetalation of To^{M} (ca. –17 ppm). Overall, the ^{1}H and ^{11}B NMR spectra associated with the To^{M} ligand in the series of organometallic species are comparable, whereas the chemical shifts for the oxazolinylborate ligand in To^{M}CoX (e.g. X = Cl, O^{t}Bu, OAc) complexes vary considerably. These data suggest that the organometallic compounds' electronic structures, which are responsible for the paramagnetic chemical shifts, are similar between simple alkyl, β-H containing alkyl, trimethylsilyl-substituted alkyl, aryl, and benzyl ligands.

Table 1. NMR Data for To^{M}CoR.

Compound	^{1}H NMR (ppm)[a]			^{11}B NMR (ppm)
	To^{M} (CH$_2$)	To^{M} (CH$_3$)	R	
To^{M}CoBn (**1**)	16.3	–12.5	34.5, –77.5, –89.0	100.4
To^{M}CH$_2$SiMe$_3$ (**2**)	15.7	–9.6	8.5	86.6
To^{M}CoPh (**3**)	16.7	–13.7	74.0, 10.6	107.7
To^{M}CoEt (**4**)	14.9	–14.5	–31.3	116.7
To^{M}Co^{n}Bu (**5**)	14.9	–14.3	14.2, –2.7	115.0
To^{M}CoMe[b] (**6**)	15.4	–12.1	Not detected	100.3
To^{M}CoCl[c]	24.9	8.4	Not applicable	–29

[a] *See experimental for Ph resonances.* [b] See reference 15. [c] See reference 16.

A single band at ~1590 cm^{-1} in the IR spectra of **1** – **6**, assigned to the oxazoline $\nu_{C=N}$, provided additional support for tridentate coordination of the To^{M} ligand to cobalt. Signals at higher frequency (~1630 cm^{-1}) associated with C=N stretching modes of non-coordinated oxazolinyl groups were not detected. In addition, the IR spectrum of **1** contained a new band at 3012 cm^{-1} that was assigned to an aromatic ν_{C-H} mode and taken as additional evidence of benzylation. This peak was distinct from the signals at 3070 and 3050 cm^{-1} present in all the compounds that were attributed to aromatic ν_{C-H} modes from the phenyl group in the To^{M} ligand. In contrast, the aromatic region in the IR spectrum of phenylcobalt **3** did not reveal new aromatic ν_{C-H} signals.

The UV-vis spectra (Figure 1 and Table S1) of **1** – **6** contained intense absorptions at ca. 350 (ε: 1400 – 3200 M^{-1}cm^{-1}) and 700 nm (ε: 1100 – 1500 M^{-1}cm^{-1}) and two weaker bands at ca. 570 (ε: 200 – 400 M^{-1}cm^{-1}) and 620 nm (ε: 200 – 450 M^{-1}cm^{-1}). The former, intense features are not detected in spectra of To^{M}CoCl and are characteristic of these organometallic complexes. The bands in the region of 500 – 650 nm were similar to those observed for To^{M}CoCl at 568 (ε = 362 M^{-1} cm^{-1}) and 635 nm (ε = 641 M^{-1} cm^{-1}) and were assigned to d←d transitions. These bands are related to the $^{4}T_1(P)\leftarrow{}^{4}A_2$ (F) transition in $[CoCl_4]^{2-}$ that split in lower symmetry. Across the organometallic compounds, the wavelengths of these d←d bands do not vary very much, further supporting the idea, from the NMR chemical shift analysis discussed above, that their electronic structures are similar. The benzyl compound **1**, which also showed unique reactivity (see below), contained an additional intense absorption at 439 nm (ε: 1964 M^{-1}cm^{-1}; see Figure 1).

A few four-coordinate tris(pyrazolyl)borate organocobalt species show similar features in their electronic spectra. For example, the spectrum of Tp^{iPr2}CoEt had four bands at 388 (1030 M^{-1}cm^{-1}), 580, 610, and 690 (810 M^{-1}cm^{-1}) nm[11] and p-tolyl Tp^{iPr2}CoC$_6$H$_4$Me contained an intense absorption at 697 nm (1304 M^{-1}cm^{-1}).[17] This intense ~700 nm absorption, however, is not a universal features of tetrahedral cobalt(II) alkyl complexes. In contrast, other tris(pyrazolyl)borate organocobalt species revealed weaker bands around 700 nm, such as Tp^{tBu,Me}CoMe (685 nm, 499 M^{-1}cm^{-1}), Tp^{tBu}CoMe (688 nm, 839 M^{-1}cm^{-1}; Tp^{tBu} = tris(3-t-butylpyrazolyl)borate), and Tp^{tBu,Me}CoEt (688 nm, 510 M^{-1}cm^{-1}).[12] Also, visible-region transitions were more intense for the chloride than for methyl, phenyl, or benzyl compounds in the tris(tert-butylthio)methyl borate cobalt(II) compounds PhTt^{t-Bu}CoX.[18, 19]

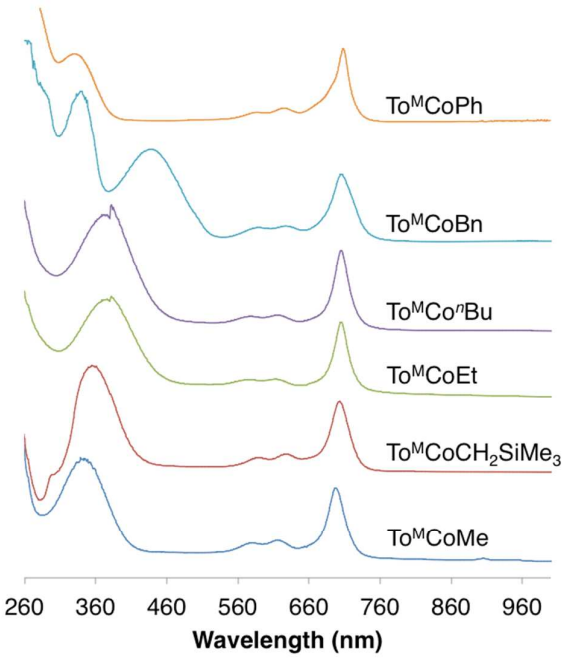

Figure 1. UV-vis spectra of To^{M}CoPh (**3**), To^{M}CoBn (**1**), To^{M}Co^{n}Bu (**5**), To^{M}CoEt (**4**), To^{M}CoCH$_2$SiMe$_3$ (**2**), and To^{M}CoMe (**6**) measured in diethyl ether.

The absorption spectra for the series of tris(oxazolinyl)borato organocobalt and heteroatom-bonded species were further studied with representative electronic structure calculations. Gas-phase models for To^{M}CoBn (**1-calc**), To^{M}CoMe (**6-calc**) and To^{M}CoCl (**To^{M}CoCl-calc**) were optimized (PBE0, 6-311+G* and Stuttgart RSC 1997)[20, 21] using the

coordinates from X-ray diffraction (see below) as initial geometries. The average Co–N distances (To^{M}CoCl, 2.02 Å; To^{M}CoCl-calc, 2.04 Å; **1**, 2.05 Å; **1-calc**, 2.06 Å; **6**, 2.05 Å; **6-calc**, 2.08 Å), B-Co-X angle (To^{M}CoCl, 171°; To^{M}CoCl-calc, 178.59°; **1**, 171.3°; **1-calc**, 173.4°; **6**, 172.8°; **6-calc**, 179.3°) and τ_4 values (To^{M}CoCl, 0.76; To^{M}CoCl-calc, 0.80; **1**, 0.75; **1-calc**, 0.75; **6**, 0.76; **6-calc**, 0.79) were in reasonably good agreement with the results from X-ray diffraction, although comparison of the latter two parameters indicated gas-phase DFT structures are more symmetrical than solid-state structures, as assessed by diffraction. The τ_4 scale for accessing distortions of four-coordinate compounds, is defined as $\tau_4 = 1$ for a T_d geometry, 0.85 for a trigonal pyramid (C_{3v}), and 0.0 for a square planar geometry.[22] The vibrational calculations for **6-calc** and To^{M}CoCl-calc contained peaks at 1667 and 1677 cm^{-1}, respectively, which corresponded to the symmetric ν_{CN} mode (the asymmetric ν_{CN} mode was low intensity). The high spin state for **1-calc** and **6-calc** were calculated to be 46 and 48 kcal/mol lower in energy than the low spin, respectively, as expected for tetrahedral cobalt(II).

TDDFT calculations on To^{M}CoCl-calc and **6-calc** revealed transitions at 602, 740 and 743 nm for both species. The intense low-energy experimental band at 697 nm in **6**, however, was not present in the TDDFT method. We previously postulated that the single configuration TDDFT approach was insufficient to correctly describe the electronic features of these compounds.[15] In fact, configuration interaction (CI) singles calculations show that the ground state wave functions of organocobalt **1-calc** and **6-calc** are distinct from that of To^{M}CoCl-calc. The ground state electronic structure of To^{M}CoCl-calc is best described by a single-reference wavefunction. In contrast, the ground state wave functions of **1-calc** and **6-calc** contain multireference character (i.e., the ground state has more than one contributing electronic configuration). The primary distinction between the To^{M}CoCl-calc compared to **1-calc** and **6-calc** is the location of two molecular orbitals with nodal planes of the phenyl ring on the To^M ligand (Figure 2) within the molecular orbital space manifold.

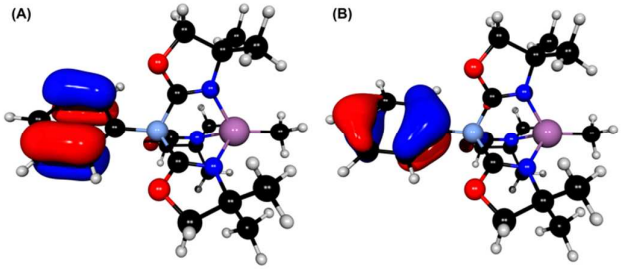

Figure 2. Three-dimensional rendering of molecular orbitals showing the nodal planes of the phenyl ring of **6-calc** calculated using configuration interaction singles.

In the To^{M}CoCl-calc system, these two orbitals are lower in energy than in **1-calc** and **6-calc**, nearly degenerate, and are both doubly occupied. In a single reference calculation for **1-calc** and **6-calc**, these two orbitals are split – one in the doubly occupied space and the other in the singly occupied space, thus creating an artificial preference of one orbital over another to be singly occupied. Multireference character in the ground state wavefunction of **6-calc** helps to explain why the excitation at 697 nm from the experimental UV-Vis was not found in earlier TDDFT calculations. The CI singles calculation of **1-calc** contain an excited state (3rd excited state) with an energy difference from the ground state corresponding to an excitation at 661 nm. The excitation is from a doubly occupied bonding orbital to a singly occupied anti-bonding orbital centered on the cobalt. The orbitals involved in this excitation are mostly, but not purely, d orbitals and include contributions from the oxazolines and the methyl group; however, the d orbitals have the largest changes in electron density. Thus, this transition is identified as essentially a d←d transition. The conclusions from CI calculations on **1-calc** are also consistent with those from the study of **6-calc**.

Solution-phase magnetic moments of compounds **1** – **6** range from 4.0 to 4.9 μ_B (Table S1) at room temperature, measured using Evans method, and were consistent with high-spin cobalt(II) (S = 3/2, spin-only μ_{eff} = 3.87 μ_B) and the calculated electronic structures. With the exception of To^{M}CoPh, the effective magnetic moments are within the range reported for other pseudo-tetrahedral organocobalt(II) complexes.[10, 12] In high spin, tetrahedral cobalt(II) with an $e^4t_2^3$ configuration, orbital contributions to the magnetic moment are expected to be quenched in the ground state, but low-lying excited state mixing results in μ_{eff} ranging from 4 – 5 μ_B.[23] EPR spectra for **1** – **6** (Figures S62) all contain striking eight-line patterns resulting from hyperfine coupling (54 G) to the ^{59}Co center (I = 7/2). Other four-coordinate {κ^3-To^M}Co^{II} species, namely To^{M}CoCl and To^{M}CoO^{t}Bu, produced rhombic signals that were devoid of hyperfine coupling.

The spectroscopically assigned structures of compounds **1** – **6** are validated by X-ray diffraction studies of single crystals (Figures 3 – 5 and ESI). The molecular structures are similar to previously reported tris(oxazolinyl)borate magnesium (d^0) and zinc (d^{10}) organometallic compounds.[24, 25] In each cobalt complex, the tris(oxazolinyl)borate ligand is coordinated in a tridentate motif, and the To^M and alkyl or aryl ligands provide a distorted tetrahedral geometry for the cobalt centers (τ_4 = 0.75 – 0.82), which is similar to To^{M}MgMe (τ_4 = 0.75) and To^{M}ZnMe (τ_4 = 0.76). The ∠B–M–Me in To^{M}MgMe (172.89°), To^{M}ZnMe (174.74) and To^{M}CoMe (172.83°) are similar. The τ_4 scale, the ∠N–Co–C angles, and the B–M–C angles describe similar distortions of the alkyl ligand away from the C_3 axis in the {κ^3-To^M}M motif. That is, the three unpaired d electrons in the high spin cobalt(II) compounds appear to have little consequence on the coordination geometry. In addition, the Co–C distances in compounds **1** – **6** vary only from 1.994(2) (**6**) to 2.023(2) Å for **1** (see Table S2). The Co–N interatomic distances are also similar across the series, varying from 2.019(2) to 2.062(3) Å. That is, the similar electronic features identified by UV-vis, EPR, and NMR spectroscopies are also reflected in similar structural parameters.

Complexes **1** – **6** persist in solution at elevated temperatures (in the absence of air and moisture). For example, ethyl and butyl compounds **4** and **5** do not eliminate

detectable quantities of ethylene or butene, respectively, after thermal treatment at 120 °C despite the possibility for β-hydrogen elimination or Co–C bond homolysis. Similar resistance toward β-hydrogen elimination in a bulkier tris(pyrazolyl)borato cobalt ethyl, Tp^{iPr2}CoEt, was attributed to its high spin electronic configuration.[10, 26] Products of Co–C bond homolysis, such as ethane or butane, are also not formed.

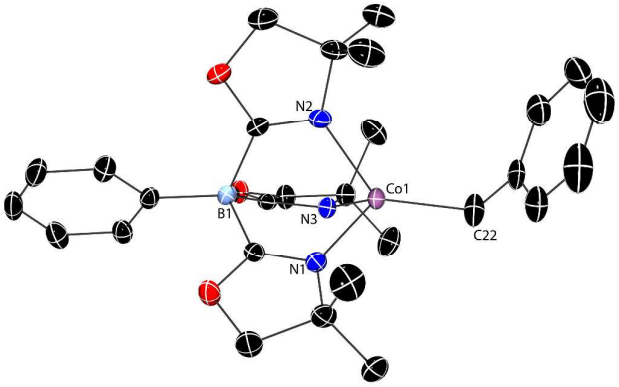

Figure 3. Thermal ellipsoid diagram of To^{M}CoBn (**1**) with ellipsoids plotted at 50% probability. H atoms are omitted for clarity. Selected interatomic distances (Å) and angles (°): Co1–C22, 2.023(2); Co1–N1, 2.040(1); Co1–N2, 2.055(1); Co1–N3, 2.041(1); N1–Co1–C22, 122.94(6); N2–Co1–C22, 131.33(6); N3–Co1–C22, 116.37(6); N1–Co1–N2, 91.68(5); N1–Co1–N3, 94.00(5); N2–Co1–N3, 91.00(5), B1–Co1–C22, 171.27(6).

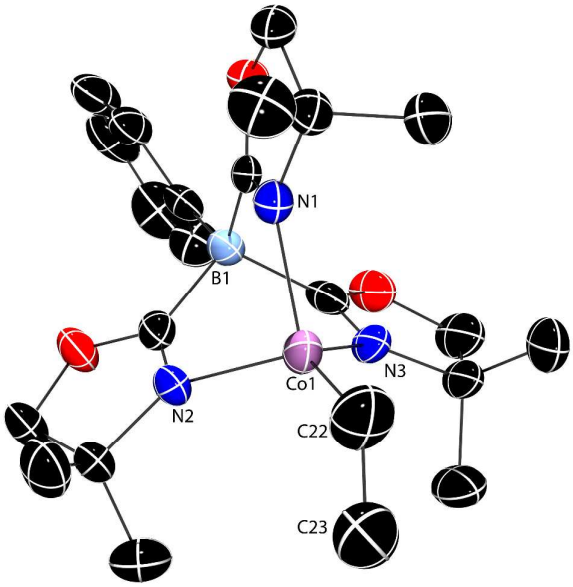

Figure 4. Thermal ellipsoid plot of To^{M}CoEt (**4**) with ellipsoids rendered at 50% probability. Hydrogen atoms are omitted for clarity. Selected interatomic distances (Å) and angles (°): Co1–C22, 1.980(3); Co1–N1, 2.046(2); Co1–N2, 2.045(2); Co1–N3, 2.046(2); N1–Co1–C22, 119.7(1); N2–Co1–C22, 126.9(1); N3–Co1–C22, 125.2(1); N1–Co1–N2, 92.52(9); N1–Co1–N3, 91.07(9); N2–Co1–N3, 91.77(9); B1–Co1–C22, 175.4(1).

Crude samples of **2** – **5**, apparently pure and To^{M}CoCl-free as determined by ^{1}H NMR, ^{11}B NMR and UV-vis spectroscopy, revealed small amounts of To^{M}CoCl (<10%) as a contaminant after addition of CO. In contrast, reactions of either **1** or **6** and CO or CO_2 provide acyl or carboxylate products that are free of To^{M}CoCl impurity, implying that the source of To^{M}CoCl is not present in either the cobalt benzyl or methyl samples. Ultimately, recrystallization of organocobalt(II) species **2** – **5** afforded isolable organometallic species that did not generate detectable To^{M}CoCl in subsequent reactions.

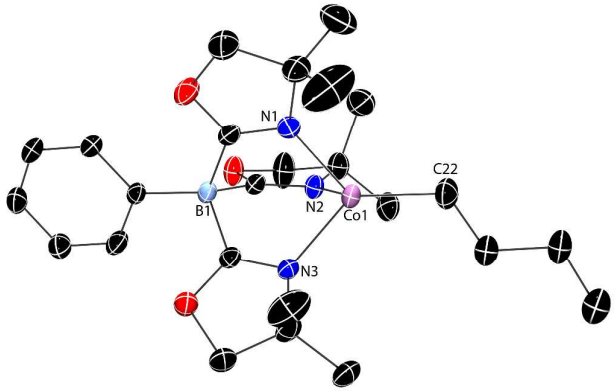

Figure 5. Thermal ellipsoid plot of To^{M}Co^{n}Bu (**5**) with ellipsoids rendered at 50% probability. H atoms are omitted for clarity. Selected interatomic distances (Å) and angles (°): Co1–C22, 2.010(4); Co1–N1, 2.046(2); Co1–N2, 2.047(2); Co1–N3, 2.054(3); N1–Co1–C22, 121.4(1); N2–Co1–C22, 124.4(1); N3–Co1–C22, 126.3(1); N1–Co1–N2, 91.2(1); N1–Co1–N3, 91.5(1); N2–Co1–N3, 92.4(1), B1–Co1–C22, 176.9(1).

Carbonylation of To^{M}CoR.

Complexes **1** – **6** rapidly react with CO (1 atm) in benzene-d_6 at room temperature (Scheme 2), as evidenced by an immediate change from blue/green to orange, to give mixtures containing organocobalt carbonyl To^{M}CoR(CO) (**7a** – **12a**; **7**, Bn; **8**, CH_2SiMe_3; **9**, Ph; **10**, Et; **11**, ^{n}Bu; **12**, Me), acyl To^{M}CoC(=O)R (**7b** – **12b**), and acyl carbonyl To^{M}Co{C(=O)R}CO (**7c** – **12c**). Species **a**, **b**, and **c** interconvert by insertion and CO coordination, or CO dissociation and decarbonylation, and the relative amounts of **a**, **b**, and **c** present in **7** – **12** vary depending on the alkyl or aryl group, as determined by IR spectroscopy. The results from analysis of the IR spectra are summarized in equations (1) – (4) in Scheme 2. Multiple ν_{CO} and $\nu_{(C=O)R}$ in the IR spectra indicate that several species are present in each reaction mixture, whereas ^{1}H and ^{11}B NMR spectroscopy suggest only a single species is formed. Together, NMR and IR spectroscopy suggest that organocobalt carbonyl **a**, acyl **b**, and acyl carbonyl **c** species interconvert through a process that is faster than the NMR timescale and slower than the IR timescale.

Compounds **8** – **12** gave similar ^{1}H NMR spectra that contained five, broad signals from 10 to –7 ppm, which were distinct from the spectra for the organocobalt(II) starting materials. Four of the ^{1}H NMR signals were attributed to the To^{M} ligand on the basis of their consistent chemical shifts across complexes **8** – **12** (9.6, 8.1, 7.7, and –1.2 ppm). The fifth

peak was assigned to the organocobalt group on the basis of its varying chemical shift among the complexes (e.g., –0.09 ppm for the CH_2SiMe_3 group in **8**, and –7.7 ppm for the ethyl group in **10**). In contrast, the ^{1}H NMR spectrum of cobalt benzyl-derived **7** contained many (>15) signals from 82 to –28 ppm that were not readily assigned to specific moieties in the complex.

Benzene-d_6 solutions of **7 – 12** were also assayed by ^{11}B NMR spectroscopy in the presence of excess CO (1 atm). The ^{11}B NMR resonance for **8 – 12** appeared at ca. –4 ppm, which was distinct from the 87 to 116 ppm chemical shift range of organocobalt

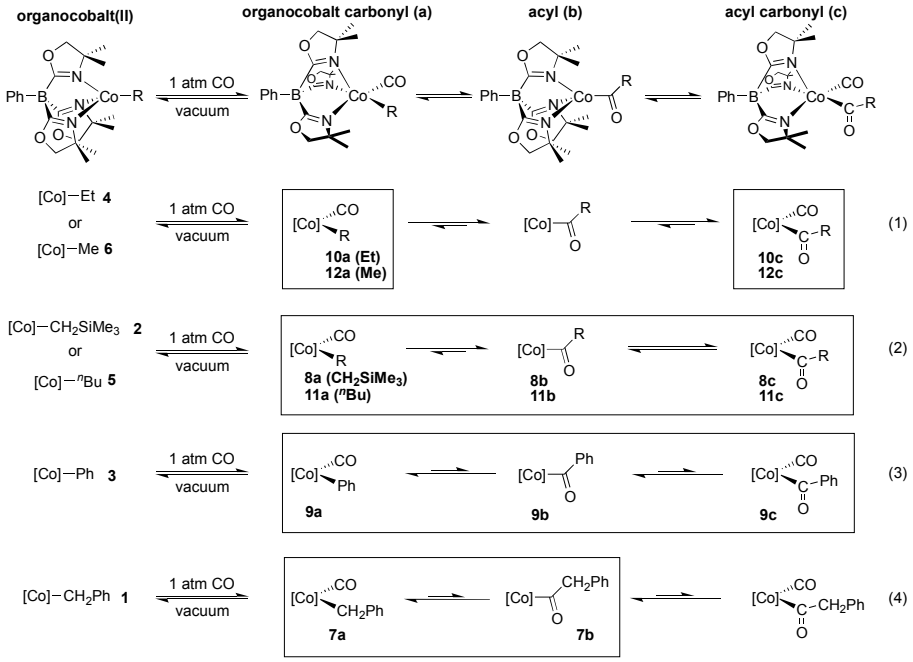

Scheme 2. Carbonylation of **1 – 6** to form interconverting mixtures of organocobalt(II) carbonyl (**a**), acyl (**b**), and acyl carbonyl (**c**) complexes. Species observed by IR spectroscopy are enclosed in boxes, and equilibrium arrows indicate favored and disfavored compounds. [Co] = κ^3-To^{M}Co.

species **1 – 6**. Unexpectedly, the 88 ppm ^{11}B NMR chemical shift for the carbonylated benzyl derivative **7** was located in the region associated with four-coordinate cobalt alkyl/aryl or five-coordinate cobalt carboxylate compounds (e.g., To^{M}CoO_2CCH_2Ph: 84 ppm).

The infrared spectra of **7 – 12**, recorded in THF solutions saturated with CO at atmospheric pressure in an ATR cell (compiled in Table 2), contained signals that were assigned to terminal carbonyl ($\nu_{C\equiv O}$, 1886 and 1973 to 1986 cm^{-1}), acyl ($\nu_{C(=O)R}$, 1650 to 1718 cm^{-1}), and the oxazoline regions (ν_{CN}: 1582 to 1594 cm^{-1}). First, the spectra of all of the compounds **7 – 12** contained a $\nu_{C\equiv O}$ band at ca. 1886 cm^{-1} (see Figure S36 – S41). This signal was the only $\nu_{C\equiv O}$ in benzyl **7**, the dominant $\nu_{C\equiv O}$ in phenyl-derived **9**, a significant signal in **8** and **11** from trimethylsilyl- and *n*-butylcobalt species, and the minor signal in ethyl **10** and methyl **12**. A higher energy $\nu_{C\equiv O}$ band, at approximately 1980 cm^{-1}, was observed for complexes **8 – 12** and appeared at the expense of the 1886 cm^{-1} signal. The 1886 and 1980 cm^{-1} peaks were assigned to organocobalt carbonyl To^{M}Co(R)CO (**a**) and acylcobalt To^{M}Co{C(=O)R}CO (**c**), respectively, on the basis of the expected increased π-back donation from organocobalt compared to acylcobalt species. This idea was supported by DFT calculations of To^{M}Co(Me)CO (**12a**) and To^{M}Co{C(=O)Me}CO (**12c**), which reproduced the trend in $\nu_{C\equiv O}$ with **12a** (2030 cm^{-1}) < **12c** (2117 cm^{-1}).

The acyl ($\nu_{C(=O)R}$) signals were less intense than $\nu_{C\equiv O}$ and appeared as one (R = CH_2SiMe_3 or Ph) or two signals (R = Et, ^{n}Bu, or Me) in the region from 1650 to 1690 cm^{-1}, but were absent for R = Bn (**7**). Instead, a band in the spectrum for **7** at 1717 cm^{-1} was assigned to terminal carbonyl-free acyl species (**b**) because the spectrum lacked the $\nu_{C\equiv O}$ band associated with **c** (see Table 2). These assignments were further supported by the IR spectra of **8**, **9**, and **11**, which contained IR signals associated with all three species **a**, **b**, and **c**.

The region from 1630 - 1500 cm^{-1} is typically associated with ν_{CN} modes of the oxazoline. The IR spectra of compounds **7 – 12** all contained an intense band from 1590 to 1600 cm^{-1}, assigned to the coordinated oxazolines. In the spectrum of ethyl **10**, a

Table 2. Infrared spectroscopic data of **7** – **12** collected in CO-saturated THF using a ZnSe crystal in ATR mode. Not detected (N.D.) in the IR spectrum.

	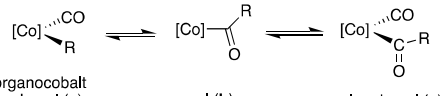 organocobalt carbonyl (**a**)		acyl (**b**)		acyl carbonyl (**c**)
R	$\nu_{C=O}$ (cm^{-1}) (**7a – 12a**)	$\nu_{(C=O)R}$ (cm^{-1}) (**7b – 12b**)	$\nu_{C=O}$ and $\nu_{C=O}$ (cm^{-1}) (**7c – 12c**)		
Bn (**7**)	1887	1716	n.d.		
CH_2SiMe_3 (**8**)	1887	1718	1973	1673	
Ph (**9**)	1886	1715	1986	1686	
Et (**10**)	1887	n.d.	1980	1667 1650	
^{n}Bu (**11**)	1887	1717	1979	1687 1662	
Me (**12**)	1887	n.d.	1984	1687 1655	

lower energy shoulder accompanied the peak at 1591 cm^{-1}, whereas a higher energy shoulder at 1630 cm^{-1} was evident in the spectrum of methyl species **12**. The shoulder in **12** was previously assigned to a weakly-coordinated oxazoline group based on the Hessian calculation of a DFT-optimized square pyramidal structure of **12c-calc** (see below).[15] Two peaks were observed at 1597 and 1556 cm^{-1} for benzyl-derived **7** and at 1594 and 1556 cm^{-1} for phenyl derived **9**. In contrast, the only notable signal in the IR spectra of trimethylsilylmethyl **8** and butyl-derived **11** within that region appeared at 1590 cm^{-1}. Based on comparison of these patterns with those for the carbonyl, we assign the 1590 cm^{-1} band to ν_{CN} in terminal carbonyl-containing **a** and **c** structures, and the 1556 cm^{-1} band to ν_{CN} in $To^{M}CoC(=O)R$ species.

The orange carbonylated compounds **7 – 12** have distinct UV-vis spectra from their blue or green starting materials. The dominating bands at 350 nm and 700 nm in the starting materials, discussed above, are absent in the carbonylated product. Instead **7 – 12** are characterized by weak signals from 700 to 500 nm (ε: 100 –170 $M^{-1}cm^{-1}$) and a strong, tailing absorption from 200 to 500 nm. In addition, compounds **7 – 12** are low spin (μ_{eff} = 2.4 – 3.4(2) μ_B) as determined by the Evans method. The magnetic moments are higher than the spin-only μ_{eff} value (1.73 μ_B) for low spin Co(II) (S = 1/2). Square pyramidal compounds, with long axial Co–N interactions, typically have magnetic moments in this range (2.1 – 2.9 μ_B) that are higher than those expected for spin-only, low-spin, square planar Co(II) complexes.[27] Alternatively, contributions from the acyl species **7b – 12b** could also result in higher-than-expected magnetic moments. This idea suggests that methyl (**12**) and ethyl (**10**) derivatives would have the lowest μ_{eff} values, because their IR spectra are dominated by the CO-coordinated species. Instead, experimental μ_{eff} values for **10** and **12** are in the middle of the series (2.7 μ_B). Despite the spectroscopic similarities between cobalt methyl and ethyl derived acyl species, as seen below, the coordination geometries of even **10c** and **12c** are not equivalent.

A pentane solution of **10** cooled to –30 °C provides X-ray quality crystals, and a single crystal diffraction study reveals the five-coordinate, acyl carbonyl form $To^{M}Co\{C(=O)Et\}CO$ (**10c**) as a square pyramidal complex (τ_5 = 0.15; Figure 6).[28] Although the oxazolines are disposed trans to either CO, an acyl, or an open coordinate site, the Co1–N1 (2.037(3) Å), Co1–N2 (2.067(2) Å) and Co1–N3 (2.050(2) Å) distances are similar to each other and to the four-coordinate tris(oxazolinyl)borato organocobalt(II) compounds described above. Related $PhTt^{tBu}Co\{C(=O)R\}CO$ (R = Me, Et, or Ph) are also square pyramidal, with similar Co–S distances for basal and apical groups.[19]

We have not been able to obtain X-ray quality crystals of any of the other species in the mixture of **10**, nor have acyl or carbonyl containing compounds of **7 – 9**, **11**, or **12** been isolated. Attempts to crystallize **12**, for example, provide either $To^{M}CoMe$ (**6**) or $To^{M}CoOAc$ (**18**, see below). The reversibility of the carbonylation of the organocobalt(II) alkyls posed challenges to the compounds' isolation. Thus, evaporation and exhaustive drying of $To^{M}Co\{C(=O)Me\}CO$ provides **6** after 24 h under dynamic vacuum, whereas complexes **9 – 11** show only

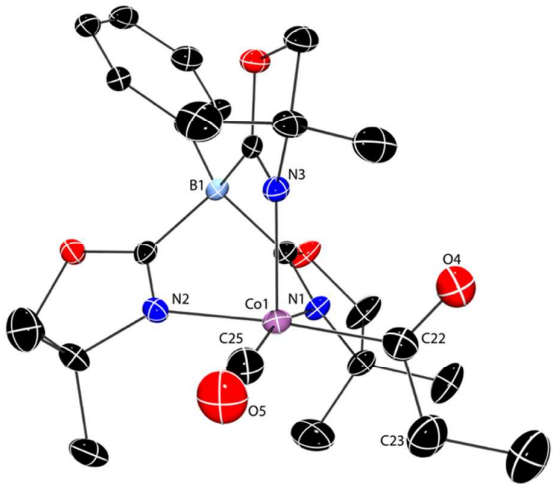

Figure 6. Thermal ellipsoid plot of $To^{M}Co\{C(=O)Et\}CO$ (**10**) plotted at 35% probability. H atoms are omitted for clarity. Selected interatomic distances (Å) and angles (°): Co1–C22 1.973(4), Co1–C25 1.751(4), Co1–N1 2.037(3), Co1–N2 2.066(3), Co1–N3 2.050(2), C22–O4, 1.207(5), C25–O5 1.156(5), N1–Co1–C22 89.7(1), N2–Co1–C22 174.0(1), N3–Co1–C22 97.1(1), N1–Co1–N2 87.0(1), N1–Co1–N3 92.6(1), N2–Co1–N3 88.1(1), C22–Co1–C25 85.5(2).

partial conversion back to **3** – **5** under these condition as assessed by ^{11}B NMR spectroscopy. Complex **8** is fully consumed upon evaporation, with $To^{M}CoCH_2SiMe_3$ as one of several other products that remain unidentified, as determined by ^{1}H and ^{11}B NMR spectroscopy.

Coupling of CO with $To^{M}CoBn$.

An entirely unique outcome occurs upon exposure of **7** to vacuum. Unlike the evaporation of **8** – **12**, which produces the corresponding organocobalt compounds **2 – 6**, a mixture was obtained from **7** that gives two signals in the ^{11}B NMR

spectrum at 86 and 87 ppm. The former signal may be from residual To^{M}CoBn(CO) in equilibrium with To^{M}CoC(=O)Bn (**7a/b**) or from To^{M}Co(CO) (**7e**, see below). The other signal, as well as a dominant peak in the ^{1}H NMR spectrum at –18 ppm, was attributed to an alkoxy ketone cobalt(II) species (**7d**, Scheme 3). The evidence for that structure is provided by X-ray diffraction studies of crystals grown from degassed solutions of To^{M}CoBn and CO (Figure 7). In that compound, one To^{M}Co, two CO, and three benzyl groups combine to form To^{M}Co{*O*,*O*-κ^2-O–C(Bn)$_2$–C(=O)Bn}.

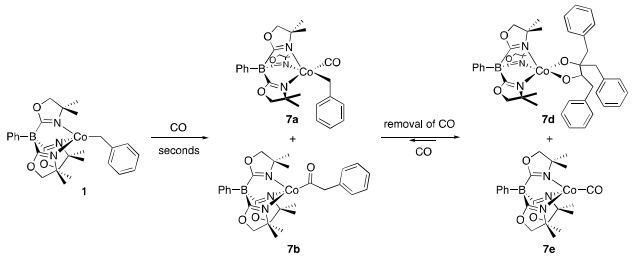

Scheme 3. Carbonylation of To^{M}CoBn (**1**) followed by removal of volatile materials provides **7d** as confirmed by X-ray crystallography and a species tentatively assigned as To^{M}CoCO (**7e**) as determined by IR spectroscopy.

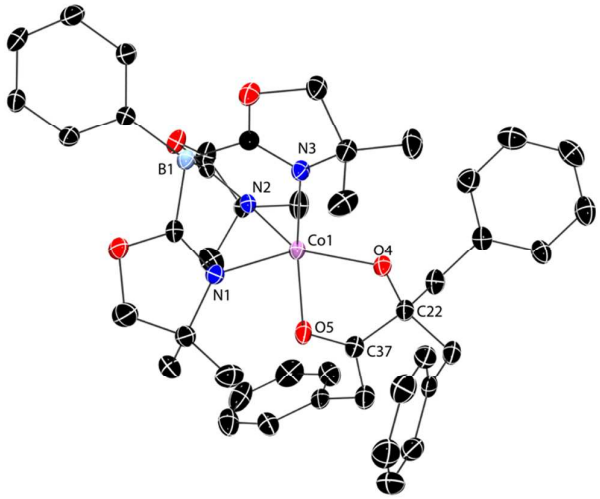

Figure 7. Thermal ellipsoid plot of **7d** at 35% probability. H atoms and a pentane molecule in the unit cell are omitted for clarity. Selected interatomic distances (Å) and angles (°): Co1–O4, 1.927(2); Co1–O5, 2.212(2); Co1–N1, 2.098(3); Co1–N2, 2.086(3); Co1–N3, 2.136(3); C22–O4, 1.386(4); C37–O5, 1.231(4); C22–C37, 1.635(4); N1–Co1–N2 88.8(1); N2–Co1–O4, 129.4(1); N1–Co1–O4, 141.4(1); N3–Co1–O5, 172.8(1); O4–Co1–O5, 77.52(9).

The coordination geometry of **7d** is distorted trigonal bipyramidal (τ_5 = 0.5). Two oxazolines (N1 and N2) and the alkoxide (O4) of the alkoxyketone are coordinated in the equatorial plane. The third oxazoline (N3) and the ketone oxygen (O5) are in axial sites (N3–Co1–O5, 172.8(1)°). The cobalt-alkoxide distance (Co1–O4, 1.972(2) Å) is shorter than that of the cobalt-ketone (Co1–O5, 2.212(2) Å), while the carbon-oxygen distances vary as expected for a ketone (O5–C37, 1.231(4) Å) and alkoxide (O4–C22, 1.386(4) Å). The distance C22–C37, between ketone and alkoxide carbon atoms, is long (1.635(4) Å). The Co–N distances (Co1–N1 2.098(3), Co1–N2 2.086(3), Co1–N3 2.136(3) Å; Co–N$_{average}$ = 2.11 Å) are all longer than other structurally characterized Co(II) complexes supported by To^{M} (e.g., Co–N$_{average}$ = 2.055 Å in **1** and 2.053 Å in To^{M}CoO$_2$CBn (**13**)). In contrast to the square pyramidal **10** whose apical Co1–N3 distance is similar to the equatorial cobalt-oxazoline distances, the axial Co1–N3 in **7d** is longer than the corresponding equatorial distances.

IR spectroscopy (KBr) of the crystalline solid obtained after evaporation of **7** contained a $\nu_{C\equiv O}$ band (1943 cm^{-1}) and $\nu_{C(=O)R}$ band (1671 cm^{-1}). The $\nu_{C(=O)R}$ band is assigned to the alkoxy ketone species **7d** while the $\nu_{C\equiv O}$ band is tentatively assigned to a reduced To^{M}CoCO (**7e**) species based upon its similar frequency to signals in Tp^{Np}CoCO ($\nu_{C\equiv O}$ = 1950 cm^{-1}; Tp^{Np} = tris(3-neopentylpyrazolyl)borate)),[29] Tp^{iPr,Me}CoCO ($\nu_{C\equiv O}$ = 1946 cm^{-1}; Tp^{iPr,Me} = tris(3-isopropyl-5-methylpyrazolyl)borate)),[30] and Tp^{iPr2}CoCO ($\nu_{C\equiv O}$ ~ 1950 cm^{-1}).[11] In these Co(I) compounds, the $\nu_{C\equiv O}$ appears at lower energy than in the cobalt(II) acyl carbonyls (e.g., Tp^{iPr2}Co{C(=O)Et}CO, $\nu_{C\equiv O}$ = 1999 cm^{-1}). Unfortunately, X-ray quality crystals of To^{M}CoCO were not obtained to support this assignment. The diagnostic ^{1}H NMR signal at –18 ppm assigned to the alkoxy ketone species **7d** disappeared upon addition of CO, and the remaining signals match those that have been assigned to **7a/b** suggesting that formation of **7d** is reversible.

Compound **7d** is remarkable, in that two molecules of carbon monoxide and three benzyl groups have been coupled into an α-alkoxyketone ligand. Compounds containing such ligands are typically synthesized by coordination of pre-formed α-hydroxyketones to metal centers.[31-33] For example, 3,4-hydroxypyridinone (3,4-HOPO) and Tp^{Ph,Me}CoCl react under basic conditions to provide Tp^{Ph,Me}Co(3,4-HOPO). Unlike trigonal bipyramidal **7d**, Tp^{Ph,Me}Co(3,4-HOPO) forms a square pyramidal solid state structure.[31]

Alternatively, the α-hydroxyketone core of the ligand is related to benzoin condensation products, although the tertiary alkoxide (which containing α-hydrogen), is unlikely to be synthesized from a benzoin-like condensation of phenylacetaldehyde and dibenzylketone. Acyl anions, however, may be generated by reaction of alkyllithium and CO in the presence of electrophiles, such as ketones, to form α-hydroxyketones at low temperature (–100 to –135 °C).[34] Acylzirconium reagents, formed from hydrozirconation followed by carbonylation, also react with aldehydes to give α-hydroxyketones.[35] In contrasting chemistry, acylzirconium species are proposed to react as electrophiles with Cp*$_2$ZrH$_2$ via hydrozirconation to give [Zr]–CH$_2$–O–[Zr].[36]

A possible pathway to generate **7d** involves the combination of a cobalt acyl and a ketone, which is suggested based on these examples with early metals (Scheme 4).

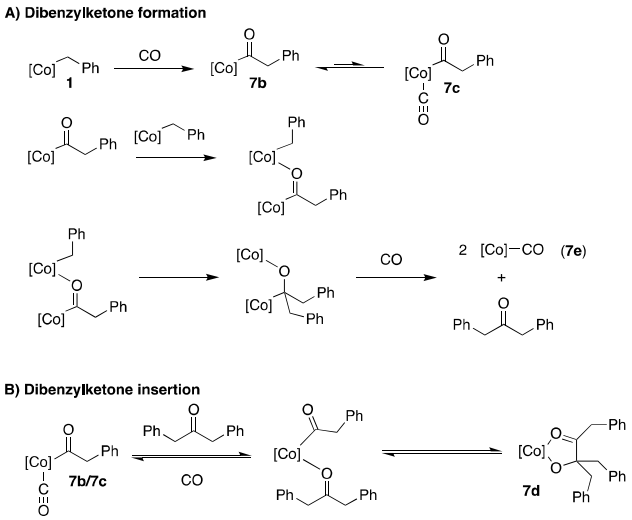

Scheme 4. Proposed formation of **7d** and **7e** by reaction of To^{M}CoBn (**1**) and CO.

The first step of the multistep process would provide dibenzyl ketone, via combination of the cobalt(II) acyl **7b** with cobalt(II) benzyl **1** to give [Co]–O–C(Bn)$_2$–[Co] in analogy to the reaction of Cp*$_2$Zr{C(=O)H}H and Cp*$_2$ZrH$_2$. Extrusion of dibenzylketone would produce two equivalents of reduced To^{M}CoCO species. Then, species **7d** could form by insertion of dibenzylketone into the cobalt-carbon bond of the cobalt acyl species (**7b**). This reaction appears to be at least partly reversed upon addition of CO, suggesting that the process requires an additional ligand to displace dibenzylketone from the coordination sphere of cobalt. Alternatively, removal of CO and crystallization provides **7d**.

That the α-alkoxyketone product is only observed in reactions of benzyl-based **1** (and not **2** – **6**) suggested the possibility of cobalt-carbon bond homolysis and trapping of To^{M}Co and benzyl radical with CO. However, no evidence of benzyl radical elimination (e.g., bibenzyl) could be obtained in solutions of **1**, and bibenzyl was not detected in reaction mixtures that produce **7d**.

Oxygenation of To^{M}Co{C(=O)R}CO and Carboxylation of To^{M}CoR.

Complexes **7** – **12** rapidly react with O_2 to form the corresponding carboxylate complexes To^{M}CoO$_2$CBn (**13**), To^{M}CoO$_2$CCH$_2$SiMe$_3$ (**14**), To^{M}CoO$_2$CPh (**15**), To^{M}CoO$_2$CEt (**16**), To^{M}CoO$_2$C^{n}Bu (**17**), and To^{M}CoO$_2$CMe (**18**) (eqn (5)).

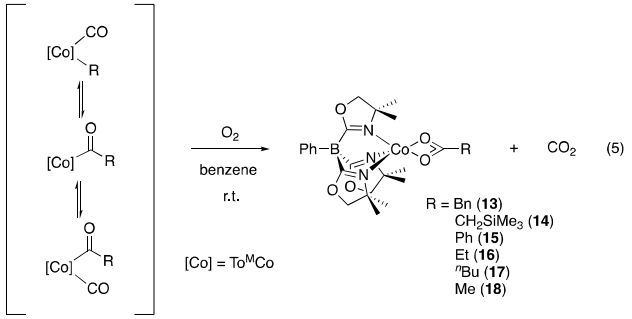

An immediate color change occurs upon addition of O_2 to the orange mixtures of **7a/b/c** – **12a/b/c** to provide purple solutions, accompanied by dramatic changes in the ^{1}H and ^{11}B NMR spectra. The ^{1}H NMR spectra of the products **14** – **18** were characteristic, with an unusual upfield chemical shift of ca. –45 ppm (18 H) assigned to the methyl from the oxazoline, as well as straightforward assignment of methylene (6 H) groups. The ^{1}H NMR spectrum of benzyl-derived **13** also revealed an intense signal at –40.8 ppm, but the methylene signal was not readily assigned, and the spectrum contained a large number of peaks. For comparison, the oxazoline methyl signals in the organocobalt starting materials appear at ca. –12 ppm (Table 1). The ^{11}B NMR spectra of **13** – **18** displayed a single signal in the region from 86 to 112 ppm, which were also distinct from the spectra measured for the exchanging carbonylated species **7** – **12** at c.a. –4 ppm.

The NMR assignments of To^{M}CoO$_2$CR are supported by their independent generation from reaction of To^{M}CoCl and MO$_2$CR (M = Na or K; R = Bn, Ph, Et, Me). The ^{1}H and ^{11}B NMR spectra, UV-Vis spectra (as THF solutions), and IR spectra (as KBr pellets) of crude samples of **13**, **15**, **16**, and **18** matched the spectra obtained from the route of eqn. (5) via sequential carbonylation and oxygenation. The cobalt carboxylate products are not easily isolated from this route, although X-ray crystals of **13** were obtained (see below). TlTo^M and CoOAc$_2$ most conveniently provide To^{M}CoOAc (**18**).[16] Alternatively, the reactions of **2** – **6** and CO_2 provide carboxylates **14** – **18**. Again, the ^{1}H and ^{11}B NMR spectra, UV-vis spectra, and IR spectra matched the spectra of materials obtained from reactions of **2** – **6** with CO and then O_2. Strangely, the reaction of benzylcobalt **1** and CO_2 affords an unidentified species whose ^{11}B NMR signal 108 ppm does not match the chemical shift of isolated **13** at 86 ppm.

Notably, direct insertion of CO_2 into the cobalt-carbon bond requires longer reaction times, which vary depending on the organocobalt species. Compound **3** reacts with CO_2 to form To^{M}CoO$_2$CPh (15) over 3 days, whereas compounds **2**, and **4** – **6** react with carbon dioxide over two weeks.

The carboxylate assignments of **13** and **15** – **18** are supported by X-ray diffraction studies of X-ray quality crystals grown from saturated pentane solutions at –40 °C (Figures 8 and 9 and Supporting Information). The crystals of **13** were obtained from reaction of To^{M}CoCl with KO$_2$Bn, **16** – **18** were isolated from reactions of To^{M}CoR (R = Et, ^{n}Bu, and Me) with CO followed by O_2, and **15** was prepared by reaction of To^{M}CoPh with CO_2. All five compounds are five coordinate and form distorted square pyramidal structures, in which one oxazoline donor is located in the apical site and the bidentante carboxylate is located in the equatorial plane. Compound **13** crystallizes with two independent molecules in the unit cell, both of which adopt distorted square pyramidal geometry (τ_5 = 0.08 and 0.34, Figure 8).[28] Two crystallizations of **18** afford different P-1 unit cells, although both molecules are distorted square pyramidal (τ_5 = 0.35 and 0.03). Compound **16** crystallizes with two, similarly distorted square pyramidal molecules in the unit cell (Figure 9, τ_5 = 0.43 and 0.33).

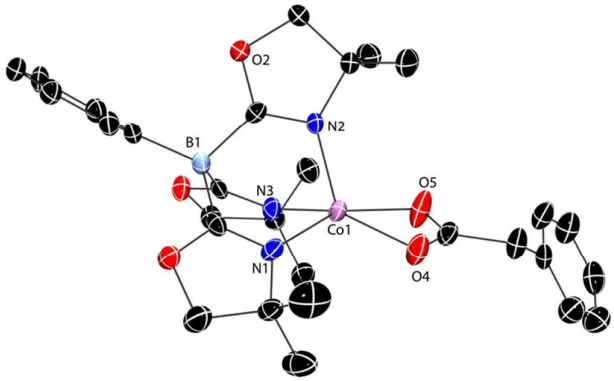

Figure 8. Thermal ellipsoid plot of $To^{M}CoO_2CBn$ (**13**) at 50% probability. A second, crystallographically-independent molecule of **13** and H atoms are omitted for clarity. Selected interatomic distances (Å) and angles (°): Co1–O4, 2.040(2); Co1–O5, 2.214(2); Co1–N1, 2.067(3); Co1–N2, 2.023(3); Co1–N3, 2.059(3); N1–Co1–N2, 92.2(1); N1–Co1–N3, 88.6(1); N2–Co1–N3, 89.9(1); N1–Co1–O5 155.4(1); N2–Co1–O4, 118.2(1); N3–Co1–O4 150.6(1); N3–Co1–O5, 102.9(1).

In general, the apical Co–N distance is shorter than the equatorial Co–N distances. An extreme example of this appears in one of the two co-crystallized molecules of the ethyl derivative **16** (τ_5 = 0.33), in which the apical Co1–N3 distance (1.837(4) Å) is considerably shorter than equatorial Co1–N1 (2.138(4) Å) and Co1–N2 (2.200(5) Å). The cobalt-oxygen interatomic distances associated with the carboxylate moiety are inequivalent in all of these structures. In the same molecule of **16**, for example, the difference between Co1–O4 (1.993(4) Å) and Co1–O5 (2.410(5) Å) is 0.42 Å. In addition, the carbon-oxygen distances in the carboxylate ligand are unequal, with C22–O4 (1.325(8) Å) much longer than C22–O5 (1.176(7) Å). These distances and differences in distances, however, are extreme in this example, whereas the difference in cobalt-oxygen distances (Co2–O9, 2.184(6) and Co2–O10, 2.005(5) Å) in the other molecule of **16** is much smaller (0.18 Å). The latter set of cobalt-oxygen distances is much more representative of the series. For example, in the two benzylcarboxylate molecules in the unit cell of **13**, the distances are Co1–O4 (2.040(3) Å) and Co1–O5 (2.214(3) Å) (Δ_{Co-O} = 0.17 Å), and Co2–O9 (2.026(3) Å) and Co2–O10 (2.214(3) Å) (Δ_{Co-O} = 0.19 Å).

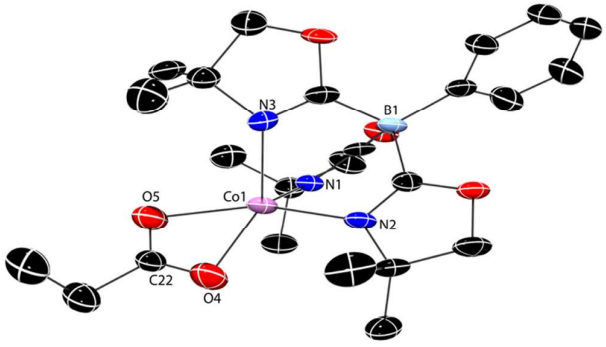

Figure 9. Thermal ellipsoid diagram illustrating one of two molecules of $To^{M}CoO_2CEt$ (**16**) at 50% probability. Hydrogen atoms are omitted for clarity. Selected interatomic distances (Å) and angles (°): Co1–O4, 1.993(4); Co1–O5, 2.410(5); Co1–N1, 2.138(4); Co1–N2, 2.200(5); Co1–N3, 1.837(4); N1–Co1–N2, 85.0(2); N1–Co1–N3, 92.3(2); N2–Co1–N3, 90.6(2); N1–Co1–O4, 140.9(2); N2–Co1–O5, 160.5(2).

As noted in the Introduction, the oxidative transformation of a metal acyl into carboxylate, either under abiotic conditions or in acetate biosynthesis, often involves reductive elimination, followed by oxidation of the metal center rather than oxygenation. Unlike the oxidative carbonylation systems that contain two cis-disposed ligands that can undergo reductive elimination, **7** – **12** do not contain hydroxide, alkoxide, or halide ligands that could reductively eliminate with the acyl group. We envisioned an possible route to reductive elimination of carboxylate through heterolytic cleavage of H–OR (R = H, alkyl, aryl) across an oxazoline-cobalt bond (Scheme 5). A related addition of HCl to $To^{M}CoCl$ can provide $\{HTo^{M}\}CoCl_2$, which contains a zwitterionic HTo^{M} ligand that coordinates to cobalt in a bidentate fashion, with the third oxazoline donor protonated at nitrogen.

This idea was tested with two experiments. First, compound **12** persists in the presence of H_2O. The ^1H NMR spectrum of mixtures containing **12** and over 10 equiv. of H_2O revealed only signals corresponding to starting materials after 30 min. This experiment did not provide evidence for protonation of an oxazoline; however, reaction of this mixture and O_2 provides compound **18** within seconds (eqn. (6)).

In a second experiment, ^{13}C-labeled **12**, generated by combination of **6** and ^{13}CO, and O_2 reacted to give two new signals in the $^{13}C\{^1H\}$ NMR spectrum at 124 and 82 ppm. The former signal was assigned to $^{13}CO_2$,[37] and the latter to

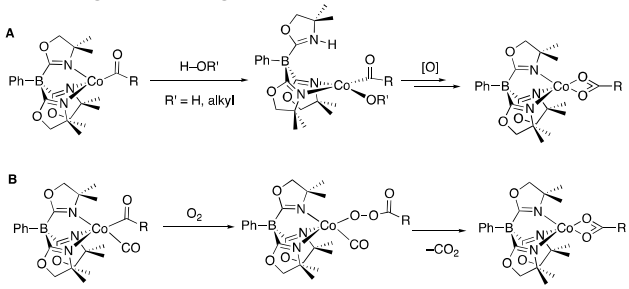

Scheme 5. Possible pathways for oxidative conversion to cobalt carboxylate via (A) protonation, elimination, and oxidation or (B) oxygenation via an acylperoxy intermediate.

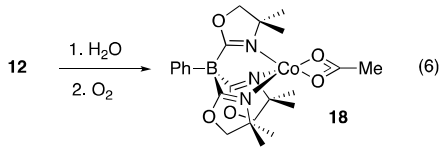

(6)

$To^{M}CoO_2{}^{13}CMe$ (**18***). The formation of CO_2 is unlikely to accompany either hydrolysis or reduction steps associated with oxidative carbonylation, and these results suggest that the cobalt acyl reacts with O_2 via oxygenation. In addition, the detection of carbon dioxide as a product of oxidation suggests that the acyl carbonyl species **12c** reacts with O_2 to provide oxygen atoms for both CO and C(=O)R ligand oxygenation. This process could involve insertion of O_2 into the [Co]–C(=O)R to

give an acylperoxy cobalt [Co]–OO–C(=O)R, which was proposed for a related oxygenation of a cobalt acyl.[17]

Conclusion

These studies of organocobalt(II) complexes **1** – **6** reveal similar spectroscopic features with variation of the hydrocarbyl ligand. Despite the distinct reaction chemistry of compound **1**, the solution-phase spectroscopic data suggests a mono-hapto benzyl coordination and similar four-coordinate structure to that found for aliphatic methyl, ethyl, and butyl complexes. While there are differences in speciation of exchanging mixtures of organocobalt carbonyl, acylcobalt, and acylcobalt carbonyl in the presence of CO and more significant changes in reactivity upon removal of CO across the series, oxygenation with O_2 consistently afford carboxylates.

First, the series of organocobalt(II) complexes **1** – **6** share similar features in their ^{1}H and ^{11}B NMR, EPR, and UV-Vis spectra that suggest similar electronic structures. Particularly, intense absorptions at ca. 350 and 700 nm in the UV-Vis spectra are a general feature of tetrahedral alkyl and aryl To^{M}Co(II) complexes that distinguishes them from other four-coordinate compounds lacking a cobalt-carbon bond, including To^{M}CoOAc, To^{M}Co*O*t*B*u or To^{M}CoCl.

Reactions of **1** – **6** and CO afford mixtures containing organocobalt carbonyl, cobalt acyl, and/or cobalt acyl carbonyl species that interconvert. The speciation of the mixture varies, depending upon the R group with only the benzyl **7** favoring organocobalt carbonyl and cobalt acyl, whereas ethyl **10** and methyl **12** favor cobalt acyl and its carbonyl adduct. The spontaneous formation of α-alkoxyketone ligand is postulated to involve coupling of dibenzylketone and cobalt acyl. We are currently pursuing related reactions of acyl species and ketones as a promising synthetic route to a range of substituted derivatives, as well as providing evidence that supports or rules out the proposed pathway. We also note that the carboxylate products of oxidation could be exchanged for organometallic ligands via transmetalation reactions; we are also investigating these reactions toward catalytic oxygenative hydrocarbon functionalizations.

Experimental

Materials and methods.

All reactions were performed using standard Schlenk techniques under an atmosphere of dry argon. Benzene and diethyl ether were dried and deoxygenated using an IT PureSolv system. Benzene-d_6 was degassed with freeze-pump-thaw cycles, heated to reflux over a Na/K alloy, and then vacuum transferred. To^{M}CoCl, To^{M}CoMe (**6**), To^{M}Co{C(=O)Me}CO (**12**), and To^{M}CoOAc (**18**) were synthesized or generated following the reported procedures.[15, 16] ^{1}H and ^{11}B NMR spectra were collected on a Bruker Avance III 600 spectrometer. ^{11}B NMR spectra were referenced to an external sample of $BF_3{\cdot}Et_2O$. Infrared spectra were measured on a Bruker Vertex 80 FTIR spectrometer. EPR spectra were obtained on an X-band Elexsys 580 FT- EPR spectrometer in continuous wave mode. UV-Vis spectra were recorded on an Agilent 8453 UV-vis spectrophotometer. Magnetic moments were measured by Evans Method at room temperature. Elemental analyses were performed using a Perkin-Elmer 2400 Series II CHN/S. Single crystal X-ray diffraction data was collected on an APEX II diffractometer.

Synthetic procedures

To^{M}CoBn (1). To^{M}CoCl (0.147 g, 0.308 mmol) and KBn (0.067g, 0.515 mmol) were stirred in tetrahydrofuran (10 mL) for 2 h. The green solution was evaporated to dryness under vacuum, the residue was extracted with benzene (10 mL), and the extracts were dried *in vacuo* to afford To^{M}CoBn as a green solid (0.129 g, 0.242 mmol, 79%). ^{1}H NMR (benzene-d_6, 600 MHz): δ 34.47 (s, 2 H), 16.33 (s, 6 H, CNCMe$_2$*CH*$_2$O), 14.90 (s, 2 H), 10.96 (s, 2 H), 9.14 (s, 1 H), –12.46 (s, 18 H, CNC*Me*$_2$CH$_2$O), –77.45 (s, 1 H), –89.01 (s, 1 H). ^{11}B NMR (benzene-d_6, 128 MHz): δ 100.4. IR (KBr, cm^{-1}): ν 3072 (w), 3046 (w), 3012 (w), 2966 (m), 2926 (m), 2897 (m), 2869 (m), 1701 (w), 1588 (s, ν_{CN}), 1482 (m), 1459 (m), 1384 (m), 1366 (m), 1351 (m), 1271 (m), 1194 (m) 1160 (m), 1027 (m), 1008 (m), 963 (m). UV-vis (Et$_2$O): λ_{max} = 339 (ε 3205 M^{-1}cm^{-1}), 439 (ε 1964 M^{-1}cm^{-1}) 589 (ε 332 M^{-1}cm^{-1}), 628 (ε 365 M^{-1}cm^{-1}), 704 (ε 1444 M^{-1}cm^{-1}). μ_{eff} (benzene-d_6) = 4.2(7) μ_B. Anal. Calcd. for $C_{28}H_{36}BCoN_3O_3$: C, 63.17; H, 6.82; N, 7.89. Found: C, 62.71; H, 7.10; N, 8.19. Mp 151 – 153°C, dec.

To^{M}CoCH$_2$SiMe$_3$ (2). LiCH$_2$SiMe$_3$ (0.041 g, 0.44 mmol) dissolved in pentane (1 mL) was added dropwise to a solution of To^{M}CoCl (0.150 g, 0.31 mmol) in tetrahydrofuran (3 mL) cooled to –78 °C. The purple reaction mixture was stirred for 15 min. at –78 °C, warmed to room temperature, and then stirred for an additional 45 min. The solvent was evaporated, and the residue was extracted with benzene. Evaporation of benzene afforded To^{M}CoCH$_2$SiMe$_3$ as a blue solid (0.161 g, 0.30 mmol, 97% yield). X-ray quality crystals were obtained from a saturated pentane solution at –40 °C. ^{1}H NMR (benzene-d_6, 600 MHz): δ 15.73 (s, 6 H, CNCMe$_2$*CH*$_2$O), 12.72 (s, 2 H, C$_6$H$_5$), 10.08 (s, 2 H, C$_6$H$_5$), 8.54 and 8.48 (s, 10 H, CH$_2$Si*Me*$_3$, *p*-C$_6$H$_5$), –9.58 (s, 18 H, CNC*Me*$_2$CH$_2$O). ^{11}B NMR (benzene-d_6, 128 MHz): δ 86.6. IR (KBr, cm^{-1}): ν 2966 (m), 2892 (m), 1586 (s, ν_{CN}), 1490 (m), 1462 (m), 1434 (m), 1386 (m), 1366 (m), 1275 (m), 1251 (m) 1195 (m), 1159 (m), 1020 (m), 1001 (m), 966 (m). UV-vis (Et$_2$O): λ_{max} = 355 (ε 2228 M^{-1}cm^{-1}), 591 (ε 374 M^{-1}cm^{-1}), 628 (ε 448 M^{-1}cm^{-1}), 703 (ε 1495 M^{-1}cm^{-1}). μ_{eff} (benzene-d_6) = 4.9(3) μ_B. Anal. Calcd. for $C_{25}H_{40}BCoN_3O_3Si$: C, 56.82; H, 7.63; N, 7.95. Found: C, 56.26; H, 7.72; N, 7.54. Mp 234 – 235 °C, dec.

To^{M}CoPh (3). Phenyllithium (1.8 M in dibutyl ether, 0.250 mL, 0.45 mmol) was added dropwise to a solution of To^{M}CoCl (0.151 g, 0.317 mmol) in THF (3 mL) cooled to –78 °C. The dark blue reaction mixture was stirred for 15 min. at –78 °C, warmed to room temperature, and stirred for an additional 45 min. The solvent was evaporated, and the residue was extracted with benzene. Evaporation of benzene provided To^{M}CoPh as a blue solid (0.119 g, 0.230 mmol, 73% yield). X-ray quality crystals were obtained from pentane solutions

cooled to –40 °C. ^{1}H NMR (benzene-d_6, 600 MHz): δ 73.95 (s, 1 H), 16.73 (s, 6 H, CNCMe$_2$CH_2O), 15.74 (s, 2 H, C$_6$H$_5$), 11.30 (s, 2 H, C$_6$H$_5$), 10.61 (s, 1 H, *p*-C$_6$H$_5$), 9.42 (s, 1 H, *p*-C$_6$H$_5$), –13.68 (s, 18 H, CNC*Me*$_2$CH$_2$O). ^{11}B NMR (benzene-d_6, 128 MHz): δ 107.7. IR (KBr, cm^{-1}): ν 3042 (m), 2967 (m), 2927 (m), 2890 (m), 2869 (m), 1582 (s, ν_{CN}), 1494 (m), 1461 (m), 1433 (m), 1388 (m), 1368 (m), 1352 (m), 1274 (m), 1196 (m), 1159 (m), 964 (m), 951 (m). UV-vis (Et$_2$O): λ_{max} = 330 (ε 1245 M^{-1}cm^{-1}), 587 (ε 176 M^{-1}cm^{-1}), 625 (ε 252 M^{-1}cm^{-1}), 708 (ε 1333 M^{-1}cm^{-1}). μ_{eff} (benzene-d_6) = 4.0(1) μ_B. Anal. Calcd. for $C_{27}H_{34}BCoN_3O_3$: C, 62.57; H, 6.61; N, 8.11. Found: C, 63.05; H, 6.81; N, 7.75. Mp 194 – 197 °C, dec.

To^{M}CoEt (4). Ethyllithium (0.5 M in a mixture of benzene and cyclohexane, 0.880 mL, 0.44 mmol) was added dropwise to a solution of To^{M}CoCl (0.150 g, 0.31 mmol) in THF (3 mL) cooled to –78 °C. The purple reaction mixture was stirred for 15 min. at –78 °C, warmed to room temperature, and stirred for an additional 45 min. Evaporation of volatiles, extraction of the solid residue with benzene, and evaporation of the benzene afforded To^{M}CoEt as a green solid (0.114 g, 0.24 mmol, 77% yield). X-ray quality crystals were obtained from pentane at –40 °C. ^{1}H NMR (benzene-d_6, 600 MHz): δ 15.95 (s, 2 H, C$_6$H$_5$), 14.85 (s, 6 H, CNCMe$_2$CH_2O), 11.33 (s, 2 H, C$_6$H$_5$), 9.42 (s, 1 H, *p*-C$_6$H$_5$), –14.45 (s, 18 H, CNC*Me*$_2$CH$_2$O), –31.31 (s, 1 H, CH$_2$CH_3). ^{11}B NMR (benzene-d_6, 128 MHz): δ 116.7. IR (KBr, cm^{-1}): ν 3078 (w), 3045 (w), 2967 (m), 2929 (m), 2895 (m), 2870 (m), 2837 (m), 1592 (s, ν_{CN}), 1495 (m), 1461 (m), 1434 (m), 1385 (m), 1366 (m), 1351 (m), 1268 (m), 1193 (m), 1159 (m), 1101 (w), 1017 (w), 961 (m). UV-vis (Et$_2$O): λ_{max} = 382 (ε 1935 M^{-1}cm^{-1}), 579 (ε 268 M^{-1}cm^{-1}), 615 (ε 286 M^{-1}cm^{-1}), 705 (ε 1255 M^{-1}cm^{-1}). μ_{eff} (benzene-d_6) = 4.1(6) μ_B. Anal. Calcd. for $C_{23}H_{34}BCoN_3O_3$: C, 58.74; H, 7.29; N, 8.94. Found: C, 58.83; H, 7.07; N, 8.64. Mp 179 – 181°C, dec.

To^{M}Co^{n}Bu (5). To^{M}CoCl (0.155 g, 0.33 mmol) was dissolved in THF (3 mL), cooled to –78 °C, and *n*-butyllithium (2.5 M in hexanes, 0.19 mL, 0.48 mmol) was added in a dropwise fashion. The dark purple reaction mixture was stirred at –78 °C for 15 min., warmed to room temperature, and stirred for an additional 45 min. THF was removed *in vacuo*, the residue was extracted with benzene, and benzene was evaporated to afford To^{M}Co^{n}Bu as a dark green solid (0.100 g, 0.20 mmol, 61% yield). X-ray quality crystals were obtained from pentane cooled to –40 °C. ^{1}H NMR (benzene-d_6, 600 MHz): δ 15.91 (s, 2 H, C$_6$H$_5$), 14.88 (s, 6 H, CNCMe$_2$CH_2O), 14.21 (s, 2 H, (CH$_2$)$_3$CH$_3$), 11.34 (s, 2 H, C$_6$H$_5$), 9.47 (s, 1 H, *p*-C$_6$H$_5$), –2.67 (s, 3 H, (CH$_2$)$_3$CH_3), –14.31 (s, 18 H, CNC*Me*$_2$CH$_2$O). ^{11}B NMR (benzene-d_6, 128 MHz): δ 115.0. IR (KBr, cm^{-1}): ν 3083 (w), 3047 (w), 2966 (m), 2928 (m), 2890 (m), 2871 (m), 1587 (s, ν_{CN}), 1495 (m), 1462 (m), 1434 (m), 1386 (m), 1368 (m), 1351 (m), 1271 (m), 1198 (m), 1159 (m), 1104 (w), 1025 (m), 995 (m). UV-vis (Et$_2$O): λ_{max} = 382 (ε 1679 M^{-1}cm^{-1}), 576 (ε 406 M^{-1}cm^{-1}), 613 (ε 422 M^{-1}cm^{-1}), 705 (ε 1291 M^{-1}cm^{-1}). μ_{eff} (benzene-d_6) = 4.5(2) μ_B. Anal. Calcd. for $C_{25}H_{38}BCoN_3O_3$: C, 60.26; H, 7.69; N, 8.43. Found: C, 60.25; H, 7.37; N, 8.32. Mp 244 – 246°C, dec.

To^{M}CoO$_2$CBn (13). Compound **7** was generated from To^{M}CoBn (0.038 g, 0.072 mmol) and CO. The CO was removed under reduced pressure, and O_2 (1 atm) was added to give a purple solution. The volatiles were evaporated in vacuo yielding To^{M}CoO$_2$CBn as a purple solid (0.038 g, 0.066 mmol, 92% yield). ^{1}H NMR (benzene-d_6, 600 MHz): δ 49.61, 32.02, 28.01, 23.86, 23.64, 17.32, 13.17, 10.93, 9.68, –40.84. ^{11}B NMR (benzene-d_6, 128 MHz): δ 86.4. IR (KBr, cm^{-1}): ν 3080 (w), 3040 (w), 2964 (m), 2928 (m), 2891 (m), 1667 (m), 1591 (s, ν_{CN}), 1517 (m), 1495 (m), 1462 (m), 1402 (m), 1367 (m), 1351 (m), 1275 (m), 1196 (m), 1160 (m), 1126 (m), 1095 (m), 1029 (m), 961 (m). UV-vis (THF): λ_{max} = 663 (ε: 200 M^{-1}cm^{-1}). μ_{eff} (benzene-d_6) = 4.7(2) μ_B. Anal. Calcd. for $C_{29}H_{36}BCoN_3O_5$: C, 60.43; H, 6.30; N, 7.29. Found: C, 60.09; H, 6.30; N, 6.89. Mp 230 – 232 °C.

To^{M}CoO$_2$CCH$_2$SiMe$_3$ (14). To^{M}CoCH$_2$SiMe$_3$ (0.046 g, 0.092 mmol) was dissolved in toluene (2 mL), the headspace was removed in vacuo, and then CO (1 atm) was introduced. An immediate color change from green to orange was observed. Evacuation of CO followed by introduction of O_2 (1 atm) resulted in a color change from orange to purple. Toluene was evaporated in vacuo to afford To^{M}CoO$_2$CCH$_2$SiMe$_3$ as a purple solid (0.043 g, 0.075 mmol, 82% yield). ^{1}H NMR (benzene-d_6, 600 MHz): δ 208.77 (s, 2 H, O$_2$CCH_2SiMe$_3$), 37.30 (s, 2 H, C$_6$H$_5$), 19.31 (s, 2 H, C$_6$H$_5$), 16.20 (s, 1 H, *p*-C$_6$H$_5$), 15.92 (s, 9 H, O$_2$CCH$_2$Si*Me*$_3$), 11.34 (s, 6 H, CNCMe$_2$CH_2O), –49.53 (s, 18 H, CNC*Me*$_2$CH$_2$O). ^{11}B NMR (benzene-d_6, 128 MHz): δ 113.2. IR (KBr, cm^{-1}): ν 3080 (w), 3049 (w), 2965 (m), 2929 (m), 2896 (m), 2872 (m), 1595 (s, ν_{CN}), 1520, 1464 (m), 1434 (m), 1368 (m), 1354 (m), 1273 (m), 1251 (m), 1196 (m), 1162 (m), 1104 (m), 1024 (m), 958 (m). UV-vis (THF): λ_{max} = 588 (ε: 98 M^{-1}cm^{-1}). μ_{eff} (benzene-d_6) = 4.7(2) μ_B. Anal. Calcd. for $C_{26}H_{40}BCoN_3O_5Si$: C, 54.55; H, 7.04; N, 7.34. Found: C, 54.41; H, 7.18; N, 7.26. Mp 186 – 188 °C.

To^{M}CoO$_2$CPh (15). To^{M}CoPh (0.020 g, 0.039 mmol) was dissolved in toluene (2 mL), the headspace was removed in vacuo, and then CO (1 atm) was introduced. An immediate color change from green to orange was observed. Evacuation of CO followed by introduction of O_2 (1 atm) resulted in a color change from orange to purple. Toluene was evaporated in vacuo to afford To^{M}CoO$_2$CPh as a purple solid (0.019 g, 0.034 mmol, 87% yield). ^{1}H NMR (benzene-d_6, 600 MHz): δ 48.80 (s, 2 H), 31.55 (s, 2 H), 23.34 (s, 2 H), 17.16 (s, 2 H), 14.48 (s, 1 H), 13.16 (s, 6 H, CNCMe$_2$CH_2O), 12.83 (s, 1 H), –40.00 (s, 18 H, CNC*Me*$_2$CH$_2$O). ^{11}B NMR (benzene-d_6, 128 MHz): δ 83.6. IR (KBr, cm^{-1}): ν 3074 (w), 3045 (w), 2965 (m), 2927 (m), 2893 (m), 2870 (m), 1589 (s, ν_{CN}), 1536 (m, ν_{CN}), 1496 (m), 1462 (m), 1408 (m), 1368 (m), 1352 (m), 1273 (m), 1197 (m), 1159 (m), 1101 (m), 1069 (m), 1025 (m), 962 (m), 949 (m). UV-vis (THF): λ_{max} = 587 (ε: 157 M^{-1}cm^{-1}). μ_{eff} (benzene-d_6) = 4.6(2) μ_B. Anal. Calcd. for $C_{28}H_{34}BCoN_3O_5$: C, 59.81; H, 6.09; N, 7.47. Found: C, 59.44; H, 6.03; N, 6.46. Mp 238 – 240 °C.

To^{M}CoO$_2$CEt (16). To^{M}CoEt (0.029 g, 0.062 mmol) was dissolved in toluene (2 mL), the headspace was removed in vacuo, and then CO (1 atm) was introduced. An immediate color change from green to orange was observed. Evacuation of CO followed by introduction of O_2 (1 atm) resulted in a color change from orange to purple. Toluene was evaporated in vacuo to afford To^{M}CoO$_2$CEt as a purple solid (0.024 g, 0.047 mmol, 76% yield). X-ray quality crystals were obtained from

pentane cooled to –40 °C. ^{1}H NMR (benzene-d_6, 600 MHz): δ 35.16 (s, 4 H), 33.81 (s, 2 H, C_6H_5), 18.05 (s, 2 H, C_6H_5), 15.20 (s, 1 H, C_6H_5), 12.32 (s, 6 H, CNCMe$_2$C*H*$_2$O), –43.62 (s, 18 H, CNC*Me*$_2$CH$_2$O). ^{11}B NMR (benzene-d_6, 128 MHz): δ 95.0. IR (KBr, cm^{-1}): ν 3080 (w), 3045 (w), 2965 (m), 2932 (m), 2893 (m), 2874 (m), 1588 (s, ν_{CN}), 1544 (m, ν_{CN}), 1466 (m), 1437 (m), 1387 (w), 1369 (m), 1352 (m), 1276 (m), 1199 (m), 1160 (m), 1074 (w), 1027 (w), 964 (m), 949 (m). UV-vis (THF): λ_{max} = 584 (ε: 98 M^{-1}cm^{-1}). μ_{eff} (benzene-d_6) = 4.8(2) μ_B. Anal. Calcd. for $C_{24}H_{34}BCoN_3O_5$: C, 56.05; H, 6.66; N, 8.17. Found: C, 56.25; H, 6.46; N, 8.02. Mp 174 – 176 °C.

To^{M}CoO$_2$C^{n}Bu (17). To^{M}Co^{n}Bu (0.030 g, 0.060 mmol) was dissolved in toluene (2 mL), the headspace was removed in vacuo, and then CO (1 atm) was introduced. An immediate color change from green to orange was observed. Evacuation of CO followed by introduction of O_2 (1 atm) resulted in a color change from orange to purple. Toluene was evaporated *in vacuo* to afford To^{M}CoO$_2$C^{n}Bu as a purple solid (0.032 g, 0.059 mmol, 98% yield). X-ray quality crystals were obtained from pentane cooled to –40 °C. ^{1}H NMR (benzene-d_6, 600 MHz): δ 161.09 (s, 2 H, $O_2CCH_2CH_2CH_2CH_3$), 34.53 (s, 2 H, $O_2C(CH_2)_3CH_3$), 33.72 (s, 2 H, $O_2C(CH_2)_3CH_3$), 19.24 (s, 2 H, C_6H_5), 17.93 (s, 2 H, C_6H_5), 15.08 (s, 1 H, *p*-C_6H_5), 12.27 (s, 6 H, CNCMe$_2$C*H*$_2$O), 10.83 (s, 3 H, $O_2C(CH_2)_3CH_3$), –43.55 (s, 18 H, CNC*Me*$_2$CH$_2$O). ^{11}B NMR (benzene-d_6, 128 MHz): δ 95. IR (KBr, cm^{-1}): ν 3079 (w), 3055 (w), 2963 (m), 2930 (m), 2893 (m), 2871 (m), 1595 (s, ν_{CN}), 1540 (m, ν_{CN}), 1498 (w), 1461 (m), 1437 (m), 1385 (m), 1365 (m), 1355 (m), 1316 (w), 1274 (m), 1107 (w), 1024 (w), 956 (s). UV-vis (THF): λ_{max} = 584 (ε: 101 M^{-1}cm^{-1}). μ_{eff} (benzene-d_6) = 4.3(2) μ_B. Anal. Calcd. for $C_{26}H_{38}BCoN_3O_5$: C, 57.58; H, 7.06; N, 7.75. Found: C, 56.47; H, 7.16; N, 7.43. Mp 197 – 199 °C.

Computational methods.

Density Functional Theory (DFT) optimizations were performed using NWChem[38] on **1-calc**, **6-calc**, **10c-calc**, **12a-calc**, **12c-cal**, and To^{M}CoCl-calc using the PBE0 hybrid functional,[20] the 6-311+G* basis for first and second row elements,[39] and the Stuttgart RSC 1997 effective core potential for cobalt.[21] Single-point energy calculations were also performed on both the high-spin and low-spin

Table 3. Summary of single crystal X-ray diffraction data for cobalt hydrocarbyl compounds **1** - **5**.

Compound	To^{M}CoCH$_2$Ph	To^{M}CoCH$_2$SiMe$_3$	To^{M}CoPh	To^{M}CoEt	To^{M}Co^{n}Bu
Compound label	**1**	**2**	**3**	**4**	**5**
Chemical formula	$C_{28}H_{36}BCoN_3O_3$	$C_{25}H_{40}BCoN_3O_3Si$	$C_{27}H_{34}BCoN_3O_3$,C_7H_8	$C_{23}H_{35}BCoN_3O_3$	$C_{25}H_{38}BCoN_3O_3$
CCDC	1845865	1845870	1845864	1845869	1845866
Crystal system	monoclinic	monoclinic	triclinic	monoclinic	monoclinic
a	14.3233(7)	12.2663(6)	11.2319(9)	11.683(2)	13.592(2)
b	13.3449(6)	14.2328(7)	11.442(1)	13.302(3)	11.081(1)
c	15.9647(7)	42.322(2)	14.056(1)	16.168(3)	17.801(2)
α	90	90	88.211(2)	90	90
β	114.139(1)	90.904(1)	87.338(2)	93.68(3)	95.162(2)
γ	90	90	63.393(1)	90	90
Volume	2784.7(2)	7448.0(6)	1613.33	2507.4(9)	2670.1(6)
Space group	P 2$_1$/c	P 2$_1$/n	P-1	P 2$_1$/c	P 2$_1$/c
Z	4	8	2	4	4
Reflections	7191	19203	6545	2627	6888
R	3.17	7.51	4.82	3.17	6.15

Table 4. Summary of single crystal X-ray diffraction data for cobalt alkoxyketone **7d**, acyl carbonyl **10**, and carboxylate compounds **13, 15** - **17**.

Compound	$To^{M}Co\{\kappa^2\text{-}OCBn_2C(=O)Bn\}$	$To^{M}Co\{C(=O)Et\}CO$	$To^{M}CoO_2CCH_2Ph$	$To^{M}CoO_2CPh$	$To^{M}CoO_2CEt$	$To^{M}CoO_2C^{n}Bu$
Compound label	**7d**	**10**	**13**	**15**	**16**	**17**
Chemical formula	$C_{44}H_{50}BCoN_3O_5,C_5H_{12}$	$C_{25}H_{34}BCoN_3O_5,(C_5H_{12})_{0.5}$	$C_{29}H_{36}BCoN_3O_5$	$C_{28}H_{34}BCoN_3O_5$	$C_{24}H_{34}BCoN_3O_5$	$C_{26}H_{38}BCoN_3O_5$
CCDC	1845867	1845874	1845871	1845868	1845872	1845873
Crystal system	monoclinic	triclinic	triclinic	triclinic	monoclinic	triclinic
a	10.051(8)	10.1610(8)	12.233(3)	10.3916(9)	14.271(3)	10.8101(6)
b	20.29(2)	10.5368(9)	14.313(4)	12.2557(9)	23.235(5)	11.5931(7)
c	23.00(2)	13.713(1)	17.118(5)	13.357(1)	15.881(3)	13.7312(8)
α	90	89.764(2)	74.05(2)	94.681(7)	90	90.193(3)
β	100.73(1)	78.934(2)	80.17(4)	110.553(6)	99.79(3)	112.684(2)
γ	90	81.773(2)	87.18(2)	112.444(5)	90	114.132(2)
Volume	4627(6)	1425.6(2)	2840(1)	1425.7(2)	5189(2)	1422.2(2)
Space group	P 2_1/c	P -1	P -1	P -1	P 2_1/c	P -1
Z	4	2	4	2	8	2
Reflections	5048	5032	7979	4038	6317	7665
R	3.9	4.62	4.52	4.82	6.63	3.85

configurations to determine the lowest energy spin state for each structure. DFT Hessians were performed on **6-calc**, **12a-calc**, and **12c-calc** to compute vibrational frequencies for comparison with experiment. A Time-Dependent DFT (TDDFT) calculation using implicit solvation was initially performed to calculate excited states for **6-calc**,[40] but it was determined that a more robust method allowing for multiple electronic configurations was needed due to missing excitations in the results. Gas-phase configuration interaction (CI) singles calculations were performed using the GAMESS quantum chemistry package on **6-calc** and To^{M}CoCl-calc to compute the first 25 excited states for each structure.[41]

Conflicts of interest

There are no conflicts to declare.

Acknowledgements

This research was supported by the U.S. Department of Energy, Office of Basic Energy Sciences, Division of Chemical Sciences, Geosciences, and Biosciences through the Ames Laboratory Catalysis and Chemical Physics programs. The Ames Laboratory is operated for the U.S. Department of Energy by Iowa State University under Contract No. DE-AC02-07CH11358.

References

1. Q. Liu, H. Zhang and A. Lei, *Angew. Chem. Int. Ed.*, 2011, **50**, 10788-10799.
2. D. J. Díaz, A. K. Darko and L. McElwee-White, *Eur. J. Org. Chem.*, 2007, 4453-4465.
3. S. W. Ragsdale and H. G. Wood, *J. Biol. Chem.*, 1985, **260**, 3970-3977.
4. P. A. Lindahl, *J. Biol. Inorg. Chem.*, 2004, **9**, 516-524.
5. T. C. Harrop and P. K. Mascharak, *Coord. Chem. Rev.*, 2005, **249**, 3007-3024.
6. S. W. Ragsdale, *Chem. Rev.*, 2006, **106**, 3317-3337.
7. S. W. Ragsdale and E. Pierce, *Biochim. Biophys. Acta, Proteins Proteomics*, 2008, **1784**, 1873-1898.
8. A. Haynes, in *Adv. Catal.*, eds. B. C. Gates and H. Knözinger, Academic Press, 2010, vol. 53, pp. 1-45.
9. S. S. Stahl, *Angew. Chem. Int. Ed.*, 2004, **43**, 3400-3420.
10. N. Shirasawa, M. Akita, S. Hikichi and Y. Moro-oka, *Chem. Commun.*, 1999, 417-418.
11. N. Shirasawa, T. T. Nguyet, S. Hikichi, Y. Moro-oka and M. Akita, *Organometallics*, 2001, **20**, 3582-3598.
12. J. D. Jewson, L. M. Liable-Sands, G. P. A. Yap, A. L. Rheingold and K. H. Theopold, *Organometallics*, 1999, **18**, 300-305.
13. J. L. Kisko, T. Hascall and G. Parkin, *J. Am. Chem. Soc.*, 1998, **120**, 10561-10562.
14. A. Kunishita, T. L. Gianetti and J. Arnold, *Organometallics*, 2012, **31**, 372-380.
15. R. R. Reinig, E. L. Fought, A. Ellern, T. L. Windus and A. D. Sadow, *Chem. Commun.*, 2017, **53**, 11020-11023.
16. R. R. Reinig, D. Mukherjee, Z. B. Weinstein, W. Xie, T. Albright, B. Baird, T. S. Gray, A. Ellern, G. J. Miller, A. H. Winter, S. L. Bud'ko and A. D. Sadow, *Eur. J. Inorg. Chem.*, 2016, 2486-2494.
17. S. Yoshimitsu, S. Hikichi and M. Akita, *Organometallics*, 2002, **21**, 3762-3773.
18. P. J. Schebler, B. S. Mandimutsira, C. G. Riordan, L. M. Liable-Sands, C. D. Incarvito and A. L. Rheingold, *J. Am. Chem. Soc.*, 2001, **123**, 331-332.
19. J. A. DuPont, M. B. Coxey, P. J. Schebler, C. D. Incarvito, W. G. Dougherty, G. P. A. Yap, A. L. Rheingold and C. G. Riordan, *Organometallics*, 2007, **26**, 971-979.
20. J. P. Perdew, M. Ernzerhof and K. Burke, *J. Chem. Phys.*, 1996, **105**, 9982-9985.
21. M. Dolg, H. Stoll, H. Preuss and R. M. Pitzer, *J. Phys. Chem.*, 1993, **97**, 5852-5859.
22. L. Yang, D. R. Powell and R. P. Houser, *Dalton Trans.*, 2007, 955-964.
23. R. S. Drago and R. S. Drago, *Physical methods for chemists*, Saunders College Pub., Ft. Worth, 2nd edn., 1992.
24. J. F. Dunne, D. B. Fulton, A. Ellern and A. D. Sadow, *J. Am. Chem. Soc.*, 2010, **132**, 17680-17683.

25. D. Mukherjee, R. R. Thompson, A. Ellern and A. D. Sadow, *ACS Catal.*, 2011, 698-702.
26. S. M. Bellows, T. R. Cundari and P. L. Holland, *Organometallics*, 2013, **32**, 4741-4751.
27. E. K. Barefield, D. H. Busch and S. M. Nelson, *Q. Rev. Chem. Soc.*, 1968, **22**, 457-498.
28. A. W. Addison, T. N. Rao, J. Reedijk, J. van Rijn and G. C. Verschoor, *J. Chem. Soc., Dalton Trans.*, 1984, 1349-1356.
29. J. L. Detrich, R. Konečný, W. M. Vetter, D. Doren, A. L. Rheingold and K. H. Theopold, *J. Am. Chem. Soc.*, 1996, **118**, 1703-1712.
30. J. L. Detrich, O. M. Reinaud, A. L. Rheingold and K. H. Theopold, *J. Am. Chem. Soc.*, 1995, **117**, 11745-11748.
31. F. E. Jacobsen, R. M. Breece, W. K. Myers, D. L. Tierney and S. M. Cohen, *Inorg. Chem.*, 2006, **45**, 7306-7315.
32. F. Lu, A. L. Rheingold and J. S. Miller, *Chem. Eur. J.*, 2013, **19**, 14795-14797.
33. H. S. Ahn, T. C. Davenport and T. D. Tilley, *Chem. Commun.*, 2014, **50**, 3834-3837.
34. D. Seyferth, R. M. Weinstein, R. C. Hui, W. L. Wang and C. M. Archer, *J. Org. Chem.*, 1992, **57**, 5620-5629.
35. S. Harada, T. Taguchi, N. Tabuchi, K. Narita and Y. Hanzawa, *Angew. Chem. Int. Ed.*, 1998, **37**, 1696-1698.
36. P. T. Wolczanski and J. E. Bercaw, *Acc. Chem. Res.*, 1980, **13**, 121-127.
37. G. R. Fulmer, A. J. M. Miller, N. H. Sherden, H. E. Gottlieb, A. Nudelman, B. M. Stoltz, J. E. Bercaw and K. I. Goldberg, *Organometallics*, **29**, 2176-2179.
38. M. Valiev, E. J. Bylaska, N. Govind, K. Kowalski, T. P. Straatsma, H. J. J. Van Dam, D. Wang, J. Nieplocha, E. Apra, T. L. Windus and W. A. de Jong, *Comput. Phys. Commun.*, 2010, **181**, 1477-1489.
39. R. Krishnan, J. S. Binkley, R. Seeger and J. A. Pople, *J. Chem. Phys.*, 1980, **72**, 650-654.
40. A. Klamt and G. Schuurmann, *J. Chem. Soc.; Perkin Trans.*, 1993, 799-805.
41. M. W. Schmidt, K. K. Baldridge, J. A. Boatz, S. T. Elbert, M. S. Gordon, J. H. Jensen, S. Koseki, N. Matsunaga, K. A. Nguyen, S. Su, T. L. Windus, M. Dupuis and J. A. Montgomery, *J. Comput. Chem.*, 1993, **14**, 1347-1363.

For Table of Contents: Tetrahedral cobalt(II) hydrocarbyl and CO reversibly form acylcobalt, coupling to give α-hydroxyketone compounds, or oxygenation with O_2 to cobalt(II) carboxylates.